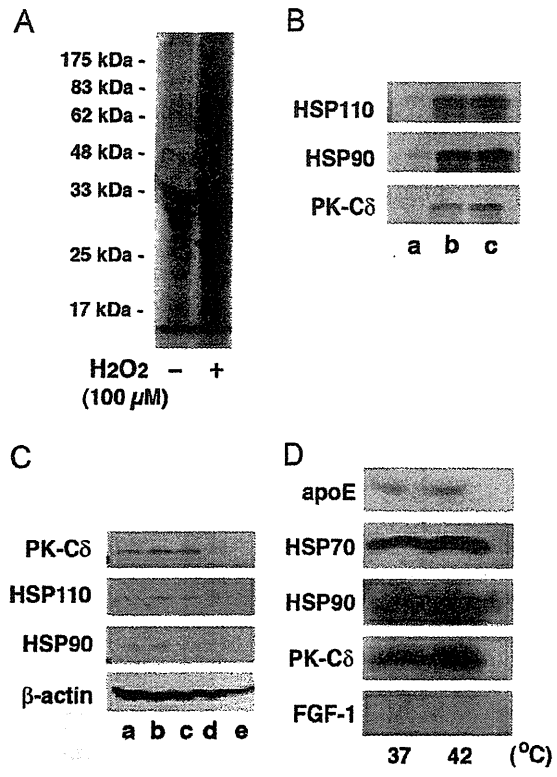

Fig. 4 – H_2O_2-induced release of cellular proteins. Rat astrocytes were incubated with [^{35}S]-methionine according to the method described in Section 4 and analyzed by SDS-PAGE and autoradiography (A). The cells were treated with or without (a) H_2O_2 (100 μM, b) or t-butyl hydroperoxide (100 μM, c) for 10 min, washed and incubated in a fresh 0.02% BSA/F-10 for 16 h. The conditioned medium was analyzed by SDS-PAGE and Western blotting to detect HSP110, HSP90, and PK-Cδ (B). The cells were treated with or without (a) 0.1% ethanol (b), 10 μM MnTMPyP/0.1% ethanol (c), 20 μM ebselen/0.1% ethanol (d) or 1 mM ascorbic acid/ 0.1% ethanol (e) for 6 h, washed and incubated in a fresh 0.02% BSA/F-10 for 16 h. The conditioned medium was analyzed by SDS-PAGE and Western blotting to detect PK-Cδ, HSP110, HSP90 and β-actin (C). The cells were incubated in 0.02% BSA/F-10 at 37 or 42 °C for 2 h and then incubated at 37 °C for 16 h in a fresh 0.02% BSA/F-10. The conditioned medium was analyzed by SDS-PAGE and Western blotting to identify apoE, HSP70, HSP90, PK-Cδ, and FGF-1 (D). All conditioned media for SDS-PAGE were prepared from the cells with 100 μg of proteins.

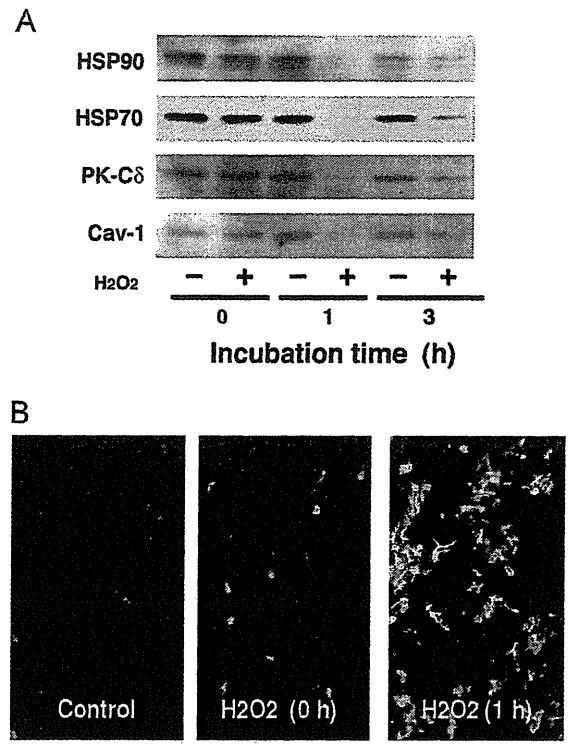

Fig. 5 – Increase in membrane permeability by H_2O_2. Rat astrocytes were treated with (+) or without (–) 100 μM H_2O_2 for 10 min, washed, and incubated in a fresh 0.02% BSA/F-10 for 0, 1, or 3 h again. The cells were treated with 2% paraformaldehyde at 4 °C for 30 min, washed with DPBS and treated with 0.1% trypsin in DPBS at 4 °C for 10 min and then at 37 °C for 10 min. After washing with DPBS, the cells (100 μg of protein) were analyzed by SDS-PAGE and Western blotting to detect HSP90, HSP70, PK-Cδ and Cav-1 (A). The cells were treated with or without (control) 100 μM H_2O_2 for 10 min in 0.02% BSA/F-10, washed with DPBS and incubated in a fresh 0.02% BSA/F-10 for 0 or 1 h. After the treatment with 2% paraform aldehyde at 4 °C for 30 min, the cells were incubated with Rhodamin-phalloidin (50-fold dilution with DPBS) at 37 °C for 2 h and observed by Fluorescence microscopy (B).

Next, we examined whether exogeneously added trypsin goes through membrane into cytosole in astrocytes treated with or without H_2O_2, followed by fixation with 2% paraformaldehyde. The treatment with exogenous trypsin decreased the levels of cytosolic proteins, such as HSP90, HSP70, PK-Cδ, and Cav-1 1 h or 3 h after the incubation of the cells with H_2O_2, whereas they remained unchanged in the cells without H_2O_2 (Fig. 5A). Rhodamin-phalloidin also flowed into the cells 1 h after H_2O_2 treatment and fixation with paraform aldehyde (Fig. 5B). These findings suggest that H_2O_2 treatment enhanced permeability of trypsin and Rhodamin-phalloidin, which enhanced proteolysis of cytoplasmic proteins and staining of cellular actin filaments, respectively. We determined the levels of HSP70 and HSP90 released from various cell types treated with H_2O_2 at various concentrations. The release of HSP90 and HSP70 from astrocytes was enhanced by H_2O_2 at concentrations of 20, 50, 100, 300, and 500 μM. However, in other cell types, the release was markedly attenuated in Balb3T3 cells, remained unchanged in bovine endothelium cells, or diminished in HepG2 cells (Fig. 6). These findings suggest that astrocytes are more sensitive to H_2O_2 in terms of the release of cytosolic proteins.

We finally examined the effect of H_2O_2 on cholesterol metabolism. The transport and incorporation of metabolically synthesized cholesterol to/in membrane fraction, especially the membrane lipid rafts (Fraction No. 3), in rat astrocytes were significantly suppressed by the treatment with H_2O_2 (Fig. 7A). The level of caveolin-1 in membrane lipid

Please cite this article as: Ito, J., et al., Enhancement of FGF-1 release along with cytosolic proteins from rat astrocytes by hydrogen peroxide, (2013), http://dx.doi.org/10.1016/j.brainres.2013.05.035

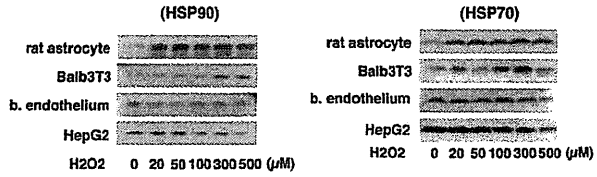

Fig. 6 – Sensitivity of various cell lines to H_2O_2. Several cell kinds, namely, astrocytes, Balb3T3, bovine endothelial cells, and HepG2 (100 μg of proteins each) were treated with H_2O_2 (0, 20, 50, 100, 300, or 500 μM) for 10 min, washed, and incubated in a fresh 0.02% BSA/F-10 for 24 h again. Each conditioned medium was prepared and analyzed by SDS-PAGE and Western blotting to detect HSP 90 and HSP70 after removal of cell debris by centrifugation at 10,000*g* for 30 min.

rafts, which was recovered with Fraction No. 3 as a marker protein of membrane lipid rafts, was reduced by oxidative stress (Fig. 7B). The transport of sphingomyelin to lipid rafts was suppressed as well. The pretreatment of rat astrocytes with lipoproteins such as LDL and HDL reduced H_2O_2-induced release of cytosolic proteins such as HSP110, HSP70, β-actin, and protein kinase Cδ (Fig. 8A). The FGF-1 release from the cells stimulated with H_2O_2 was also inhibited by the pretreatment with LDL (Fig. 8B). The digestion of cytosolic proteins by exogenous trypsin in H_2O_2-treated rat astrocytes was protected by the pretreatment with LDL (Fig. 8C). These findings suggest that the increase of membrane permeability induced by H_2O_2 results in the impairment in lipid metabolism.

3. Discussion

ApoE and apoE/HDL in the brain are generated mainly by astrocytes. We have shown that astrocytes cultured under stressful conditions such as long-term culture produce and release highly FGF-1, which stimulates apoE and apoE/HDL production in an autocrine-dependent manner (Ito et al., 2005, 2007; Ueno et al., 2002; Nishida et al., 2009). We also reported the in vivo observation that the productions of FGF-1 and apoE increase in astrocytes around a lesion of cryoinjury in the mouse brain and that FGF-1 production proceeds ahead of apoE production. Deficiency of apoE delays the healing of the injury despite of the increase in FGF-1 production (Tada et al., 2004). These findings support the hypothesis that FGF-1 is a regulator of apoE/HDL production in the brain damaged by stress and injury, and that apoE/HDL contributes to the recovery of the brain from the damage. In order to prove this hypothesis, next four subjects must be solved; (1) Whether FGF-1 is actually released by neural cells prepared from the brain under various stresses, (2) what is a mechanism underlying FGF-1 release, (3) what is a mechanism underlying apoE secretion induced by FGF-1, and (4) how apoE/HDL protects damaged brain. In this study, we attempted to examine whether FGF-1 is actually released from astrocytes under oxidative stress as common events in the case of brain damages. The experimental results in this work are summarized as follows. (1) The treatment of astrocytes with a low concentration of H_2O_2 enhanced actually release of FGF-1 without inducing apoptosis. (2) The conditioned medium

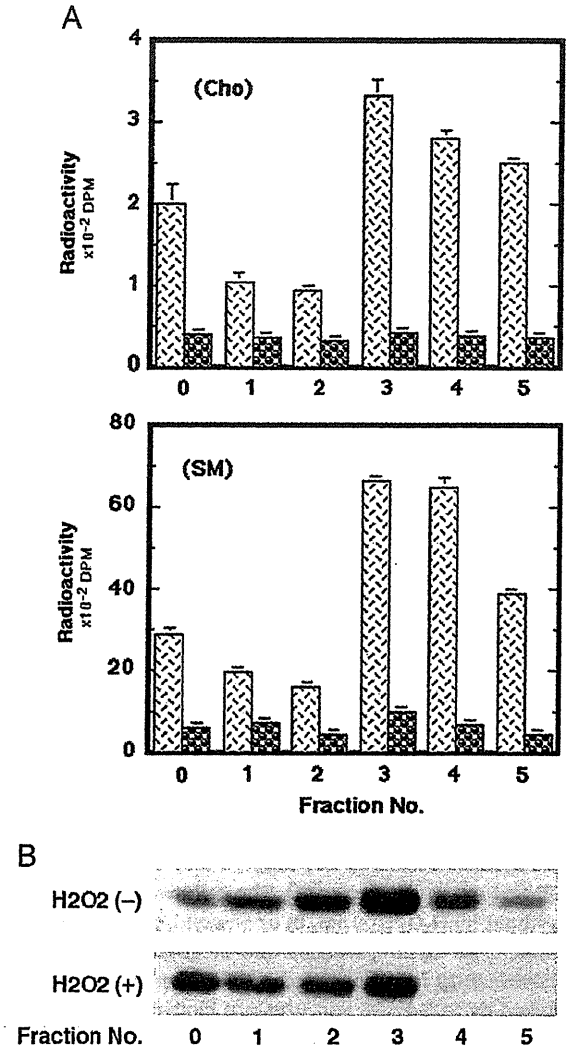

Fig. 7 – Effects of H_2O_2 on lipid synthesis and transport to de novo synthesized lipid to membrane fraction. After rat astrocytes were treated with 100 μM H_2O_2 for 10 min in 0.02% BSA/F-10, the cells were incubated with [^{14}C]-acetate (4 μCi/ml) in a fresh 0.02% BSA/F-10 for 2 h. The membrane fraction (300 μg) was prepared from the cells, sonicated and separated to 6 fractions according to the method described in Section 4. Lipid was extracted from each fraction and analyzed by TLC for cholesterol and sphingomyelin. The experiment was performed in triplicate and repeated at least once in an independent experiment. Quantitative results are expressed as mean±standard deviation (SD) (A). Proteins in each fraction were analyzed by SDS-PAGE and Western blotting for caveolin-1 using rabbit anti-caveolin-1 antibody (Santa Cruz) (B).

prepared from H_2O_2-treated astrocytes had FGF-1-like activities to enhance apoE secretion and cholesterol synthesis from/in rat astrocytes. (3) Hydrogen peroxide enhanced also the release of cytosolic proteins such as HSP70, HSP90, PK-Cδ, and β-actin from astrocytes. (4) Hydrogen peroxide suppressed lipid synthesis and lipid transport to the membrane fraction in astrocytes. (5) Exogenous LDL suppress H_2O_2-

Please cite this article as: Ito, J., et al., Enhancement of FGF-1 release along with cytosolic proteins from rat astrocytes by hydrogen peroxide, (2013), http://dx.doi.org/10.1016/j.brainres.2013.05.035

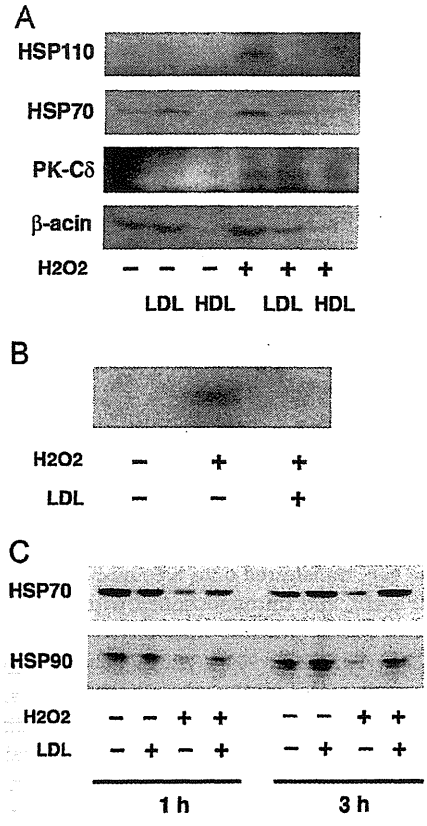

Fig. 8 – Suppression of H_2O_2-induced release of FGF-1 and cytosolic proteins by exogenous lipoproteins such as LDL and HDL. Rat astrocytes were pretreated with or without lipoproteins (50 μg of protein/ml of HDL or LDL, each) in 0.1% BSA/F-10 for 24 h. After washing 4 times with DPBS, the cells were treated with or without 100 μM H_2O_2 for 10 min in 0.02% BSA/F-10 and washed with DPBS. The cells were incubated in 0.02% BSA/F-10 for 24 h, followed by preparation of the conditioned medium. Each conditioned medium was analyzed by SDS-PAGE and Western blotting for HSP110, HSP70, protein kinase Cδ, and β-actin using specific antibodies (A). Rat astrocytes pretreated with or without exogenous LDL (50 μg of protein/ml) for 24 h were treated with or without 100 μM H_2O_2 for 10 min in 0.02% BSA/F-10, washed and incubated in a fresh 0.02% BSA/F-10 for 24 h. Heparin-sepharose was incubated with each conditioned medium at 4 °C for 16 h, washed and analyzed by SDS-PAGE and Western blotting using goat anti-FGF-1 antibody (B). After pretreatment with or without LDL (50 μg of protein/ml) for 16 h and washing with DPBS, rat astrocytes were treated with or without 100 μM H_2O_2 for 10 min and washed. The cells were incubated in a fresh 0.02% BSA/F-10 for 1 or 3 h, followed by treatment with 2% paraform aldehyde and 0.1% trypsin and analysis by SDS-PAGE and Western blotting for HSP70 and HSP90 according to the method described in Fig. 5A (C).

induced release of FGF-1 and cytosolic proteins such as HSP110 and HSP70. (6) Hydrogen peroxide enhanced the proteolysis of cytosolic proteins by exogenous trypsin, which was suppressed by the pretreatment with LDL.

Hydrogen peroxide increased the release of FGF-1 along with cytosolic proteins from astrocytes. This phenomenon was more greatly observed in the H_2O_2-treated astrocytes cultured for one month (data not shown), which increase mRNA expression, production, and intracellular accumulation of FGF-1 (Ito et al., 2005; Ueno et al., 2002). Interestingly, the treatment with H_2O_2 markedly suppressed the secretion of apoE from astrocytes, but it did not suppress the release of FGF-1, suggesting that oxidative stress may suppress the classical intracellular transport system through the ER/Golgi pathway for apoE secretion from astrocytes. From a different viewpoint, this means that FGF-1 is released from astrocytes through a pathway different from the classical secretion pathway. The release of [^{35}S]-labeled cytosolic proteins of a wide range of molecular weights following the treatment with 100 μM H_2O_2 was demonstrated in astrocytes, suggesting that the enhancement of FGF-1 release by oxidative stress depends on the mechanism nonspecific to the FGF-1 molecule in astrocytes. The release of cytosolic proteins such as HSP90 and HSP70 was actually induced in astrocytes after the treatment with at least 20 μM H_2O_2 also, whereas bovine endothelial cells and HepG2 cells showed no response to even 500 μM H_2O_2. Astrocytes seemingly have a higher performance of sensor to oxidative stress than those of other cell lines in the terms of cytosolic protein release. The release of FGF-1 may take advantage of the release of cytosolic proteins from astrocytes under oxidative stress.

FGF-1 appears to be localized in the neural tissue as a high-molecular-weight complex. The complex contains FGF-1 and p40 extravascular domain of synaptotagmin (Syn)-1, and the brain-derived FGF-1/p40 Syn-1 complex is found to be associated with the calcium-binding protein S100A13 (LaVallee et al., 1998; Landriscina et al., 2001). FGF-1 is released as a latent homodimer with the p40 extravascular domain of Syn-1, as induced by heat-shock stress (Tarantini et al., 1998). These findings indicate that FGF-1 is released as complex forms under stressful conditions. The role of the complex formation of FGF-1 in the release of FGF-1 to extracellular space under stressful condition is as yet unknown (Chapman and Davis, 1998). Graziani et al. (2006) suggested that the nonclassical pathway of release of FGF-1 and p40 Syn-1 involves the destabilization of the membrane containing acidic phospholipids. We also observed in this study that oxidative stress suppresses syntheses of lipids such as cholesterol and sphingomyelin and incorporation of de novo synthesized lipids to the lipid raft/caveolae domain in the membrane fraction. This may impair the plasma membrane functions and alter lipid raft structure. The sensitive response to oxidative stress to enhance the release of FGF-1 and cytosolic proteins may be a functional feature of astrocytes for protection of the brain from oxidative stress.

We have no information for H_2O_2-induced pore in the plasma membrane of astrocytes at present. Increasing influx of exogenous trypsin and Rhodamin-phalloidin into H_2O_2-treated astrocytes was observed only after fixation of the cells with paraform aldehyde. This suggests that paraform aldehyde treatment made pores artificially through the interaction between the plasma membrane components of H_2O_2-treated cells and paraform aldehyde, which may permit compounds go into the cells. We should study the characteristics of plasma

Please cite this article as: Ito, J., et al., Enhancement of FGF-1 release along with cytosolic proteins from rat astrocytes by hydrogen peroxide, (2013), http://dx.doi.org/10.1016/j.brainres.2013.05.035

membrane of H_2O_2-treated cells in detail as a next step to understand the relationship between oxidative stress-induced FGF-1 release and change of lipid metabolism. Oxidative stress is also associated with brain diseases such as Alzheimer's disease (Pratico and Trojanowski, 2000; Pratico and Delanty, 2000). It is expected that the FGF-1 release from astrocytes is enhanced to increase apoE/HDL production in various brain diseases, leading to protect brain tissues and functions.

4. Experimental procedure

4.1. Cell culture

Astrocytes were prepared by primary and secondary culture of brain cells from 17-day-old-Wistar rat fetuses in accordance with a method previously described (Ito et al., 1982). After the removal of the meninges, the brain was cut into small pieces and treated with 0.1% trypsin solution in Dulbecco's phosphate-buffered saline containing 0.15% glucose (0.1% trypsin/DPBS/G) for 3 min at room temperature. The trypsinized tissues were then centrifuged at 300*g* for 3 min and the resulting pellets were cultured in F-10 medium containing 10% fetal calf serum (10% FCS/F-10) at 37 °C for one week (primary culture). After the treatment with 0.1% trypsin/DPBS/G containing 1 mM ethylenediaminetetraacetic acid (EDTA), the cells were cultured in 10% FCS/F-10 for one week as a secondary culture. Mouse Balb3T3 cells, bovine endothelial cells (Sobue et al., 1999), and mouse hepatocytoma HepG2 cells were cultured in 10% FCS/DMEM.

4.2. Oxidative stress of cells

After washing three times with DPBS and incubation in 0.1% BSA/F-10 medium for 24 h, rat astrocytes and cell lines were treated with H_2O_2 (0–500 μM) or t-butyl hydroperoxide (100 μM) in 0.02% BSA/F-10 for 10 min. The cells were incubated in a fresh 0.02% BSA/F-10 for the indicated time after washing three times with DPBS. Apoptosis of rat astrocytes treated with 100 μM H_2O_2 for 0, 2, 18, or 30 h in a fresh 0.02% BSA/F-10 was examined using Vybrant™ Apoptosis Assay Kit #5 (Molecular Probes, Inc.). The cell protein was assayed with microBCA, Protein Assay Reagent Kit (Pierce). Cellular lactate dehydrogenase (LDH) level in rat astrocytes was determined using a CytoTox 96 Non-Radioactive Cytotoxicity Assay kit (promega) for the examination of H_2O_2 cytotoxicity, which was determined as the percentage of cytosolic LDH level in rat astrocytes treated with H_2O_2 with respect to that in control cells treated without H_2O_2.

4.3. Preparation of cytosol, membrane, and nucleus fraction

The subcellular fractionation of astrocytes was carried out in accordance with the modified method of Thom et al. (1977). Briefly, a cell pellet was obtained by centrifugation of cultured astrocytes at 300*g* for 10 min after washing with DPBS four times and harvesting with a rubber policeman. The cell pellet was treated with a cold hypotonic buffer, 0.02 M Tris–HCl, pH 7.5, containing a protease inhibitor cocktail (Sigma) (0.02 M Tris/protease inhibitor), for 15 min with strong mixing 25 times per 10 s every 5 min. The cell suspension was centrifuged at 1700*g* for 20 min at 4 °C to obtain the nucleus fraction as a pellet. The supernatant was centrifuged again at 367,000*g* for 30 min in a Hitachi S100AT6 rotor to obtain the cytosol as a supernatant and the membrane fraction as a pellet. The fractions of nuclei and membrane were sonicated in 1 ml of DPBS containing protease inhibitors cocktail and each aliquot of nucleus fraction and membrane fraction (50 μl each) was assayed with microBCA, Protein Assay Reagent Kit (Pierce).

4.4. Analysis of proteins in cells and conditioned medium by western blotting

The conditioned medium was treated with 10% TCA and centrifuged at 10,000*g* for 20 min to obtain a protein pellet after the removal of cell debris by centrifugation at 10,000*g* for 30 min. Proteins in the cells and the conditioned medium were separated by SDS-PAGE (0.5% SDS/10% or 12.5% polyacrylamide gel), transferred onto a Sequi-Blot™ PDVF membrane (BIO RAD), and immunostained with goat anti-FGF-1 (Santa Cruz), rabbit anti-ERK (Cell Signaling), mouse anti-phospho-ERK (Thr202/Tyr204) (Cell Signaling), mouse anti-Akt (BD), rabbit anti-phospho Akt (Thr308) (Cell Signaling), rabbit anti-MEK (Cell Signaling), mouse anti-phospho-MEK (Ser217/221) (Cell Signaling), mouse anti-HSP70, mouse anti-HSP90, mouse anti-HSP110, mouse anti-caveolin 1 (Cav-1), mouse anti-β-actin, or mouse anti-protein kinase Cδ (PK-Cδ) antibody, and rabbit anti-apoE antiserum, a generous gift from Dr. Jean Vance (University of Alberta).

4.5. Affinity isolation of proteins using heparin-Sepharose

Affinity isolation was carried out by incubation of heparin-Sepharose with the conditioned medium or the cytosol fraction at 4 °C for the indicated time. The heparin-Sepharose fraction was washed with 40 mM Tris–HCl buffer containing 60 mM octylglycoside, 0.1% SDS, 1% Triton X-100, and protease inhibitor cocktail, pH 7.4, (solubilization buffer), and washed five times with Tris–HCl-buffered saline, pH 7.4, (TBS)/protease inhibitors and subjected to SDS-PAGE. After the transfer to a Sequi-Blot PVDF membrane (PVDF, BIO-RAD), the proteins were immunostained with rabbit anti-apoE or rabbit anti-FGF-1 antiserum.

4.6. De novo synthesis and secretion of cellular proteins

After incubation in 0.1% BSA-containing DMEM medium without methionine and cysteine (0.1% BSA/DMEM (Met -, Cys -)) for 24 h, rat astrocytes were incubated with [^{35}S] methionine (20 μCi/mL, American Radiolabeled Chemicals Inc.) in 0.02% BSA/DMEM (Met -, Cys -) for 3 h and washed four times with DPBS. The cells were incubated in 0.02% BSA/F-10 for 16 h and then with 100 μM H_2O_2 for 10 min in a fresh 0.02% BSA/F-10, followed by washing four times with DPBS. After the incubation in 0.02% BSA/F-10 for 5 h, the conditioned medium, in which cell debris was removed by centrifugation at 10,000*g* for 30 min, was treated with 10% TCA and analyzed by SDS-PAGE and autoradiography.

Please cite this article as: Ito, J., et al., Enhancement of FGF-1 release along with cytosolic proteins from rat astrocytes by hydrogen peroxide, (2013), http://dx.doi.org/10.1016/j.brainres.2013.05.035

4.7. *Biosynthesis of cholesterol and phospholipids*

After washing three times with DPBS, rat astrocytes were incubated with or without 100 μM H_2O_2 in 0.02% BSA/F-10 for 10 min, washed four times with DPBS and further incubated with [^{14}C]-acetate (2–4 μCi/ml; New England Nuclei) in a fresh 0.02% BSA/F-10 for 2 h for lipid synthesis. Lipids were extracted from whole cells using hexane-isopropanol (3:2; v/v).

The lipids were analyzed by thin layer chromatography (TLC) on Silica Gel-60 plates (Merck). The radioactivities of cholesterol and sphingomyelin were determined using a liquid scintillation counter.

4.8. *Membrane lipid rafts preparation*

The membrane fraction was sonicated in 0.75 mL of 0.02 M Tris/protease inhibitor six times every 10 s at level 6 with a Taitec UP-55 homogenizer. The sonicated membrane fraction was adjusted to 30% sucrose to add 0.75 mL of 60% sucrose solution. After 1.5 mL of 10% sucrose solution was overlaid, the sample was centrifuged at 367,000*g* for 60 min and then collected from the bottom of the centrifugation tube into five solution fractions and pellet (total 6 fractions), followed by analysis by SDS-PAGE. The caveolin-1 was recovered from the Fraction No. 3 (Ito et al., 2011).

4.9. *Statistical analysis*

Each experiment was performed in triplicate and repeated at least once in an independent experiment. Quantitative results are expressed as mean±standard deviation (SD). Representative results are shown. Values were compared using Student's t-test, and a value of $p<0.05$ was considered to be statistically significant.

REFERENCES

Carreira, C.M., LaVallee, T.M., Tarantini, F., Jackson, A., Lathrop, J.T., Hampton, B., Burgess, W.H., Maciag, T., 1998. S100A13 is involved in the regulation of fibroblast growth factor-1 and P40 synaptotagmin-1 release in vitro. J. Biol. Chem. 273, 22224–22231.

Chapman, E.R., Davis, A.F., 1998. Direct interaction of a Ca2+-binding loop of synaptotagmin with lipid bilayers. J. Biol. Chem. 273, 13995–14001.

Dietschy, J.M., Turley, S.D., 2001. Cholesterol metabolism in the brain. Curr. Opin. Lipidol. 12, 105–112.

Dono, R., 2003. Fibloblast growth factors as regulators of central nervous system development and function. Am. J. Physiol. Regul. Integr. Comp. Physiol 284, R876–R881.

Eckenstein, F.P., Andersson, C., Kuzis, K., Woodward, W.G., 1994. Distribution of acidic and basic fibroblast growth factors in the mature, injured and developing rat nervous sysem. Prog. Brain Res. 103, 55–63.

Eckenstein, F.P., 1994. Fibloblast growth factors in the nervous system. J. Neurobiol. 25, 1467–1480.

Graziani, I., Bagala, C., Duate, M., Soldi, R., Kolev, V., Tarantini, F., Kumar, T.K., Doyle, A., Neivandt, D., Yu, C., Maciag, T., Prudovsky, I., 2006. Release of FGF1 and p40 synaptotagmin 1 correlates with their membrane destabilizing ability. Biochem. Biophys. Res. Com. 349, 192–199.

Ito, J.-i., Yokoyama, S., 2004. Roles of glia cells in cholesterol homeostasis in the brain. Adv. Mol. Cell Biol. 31, 519–534.

Ito, J.-i., Zhang, L.-Y., Asai, M., Yokoyama, S., 1999. Differential generation of high-density lipoprotein by endogenous and exogenous apolipoproteins in cltured fetal rat astrocytes. J. Neurochem. 72, 2362–2369.

Ito, J.-i., Nagayasu, Y., Kheirollah, A., Abe-Dohmae, S., Yokoyama, S., 2011. ApoA-I enhances generation of HDL-like lipoproteins through interaction between ABCA1 and phospholipase Cgamma in rat astrocytes. Biochim. Biophys. Acta 1811, 1062–1069.

Ito, J.-i., Nagayasu, Y., Lu, R., Kheirollah, A., Hayashi, M., Yokoyama, S., 2005. Astrocytes produce and secrete FGF-1, which promotes the production of apoE-HDL in a manner of autocrine action. J. Lipid Res. 46, 679–686.

Ito, J.-i., Kato, T., Yamanaka, Y., Kato, H., Sakazaki, Y., Lim, R., Tanaka, R., 1982. Interaction of glia maturation factor with the glial cell membrane. Brain Res. 243, 309–314.

Ito, J.-i., Nagayasu, Y., Okumura-Noji, K., Lu, R., Nishida, T., Miura, Y., Asai, K., Kheirollah, A., Nakaya, S., Yokoyama, S., 2007. Mechanism for FGF-1 to regulate biogenesis of apoE-HDL in astrocytes. J. Lipid Res. 48, 2020–2027.

Jackson, A., Friedman, S., Zhan, X., Engleka, K.A., Forough, R., Maciag, T., 1992. Heat shock induces the release of fibroblast growth factor 1 from NIH3T3 cells. Proc. Natl. Acad. Sci. USA 89, 10691–10695.

Landriscina, M., Bagala, C., Mandinova, A., Soldi, R., Micussi, I., Bellum, S., Prudovsky, I., Maciag, T., 2001. Copper induces the assembly of a multiprotein aggregate implicated in the release of fibroblast growth factor 1 in response to stress. J. Biol. Chem. 276, 25549–25557.

Larsson, H., Klint, P., Landgren, E., Claesson-Welsh, L., 1999. Fibroblast growth factor receptor-1-mediated endothelial cell proliferation is dependent on the Src homology (SH)2/SH3 domain-containing adaptor protein Crk. J. Biol. Chem. 274, 25726–25734.

LaVallee, T.M., Tarantini, F., Gamble, S., Carreira, C.M., Jackson, A., Maciag, T., 1998. Synaptotagmin-1 is required for fibroblast growth factor-1 release. J. Biol. Chem. 273, 22217–22223.

Linton, M.F., Gish, R., Hubl, S.T., Butler, E., Esquivel, C., Bry, W.I., Boyles, J.K., Wardell, M.R., Young, S.G., 1991. Phenotypes of apolipoprotein B and apolipoprotein E after liver transplantation. J. Clin. Invest. 88, 270–281.

Lu, R., Ito, J.-i., Iwamoto, N., Nishimaki-Mogami, T., Yokoyama, S., 2009. FGF-1 induces expression of LXR and production of 25-hydroxycholesterol to upregulate the apoE gene in rat astrocytes. J. Lipid Res. 50, 1156–1164.

Mashayekhi, F., Hadavi, M., Naji, M., 2010. Increased acidic fibroblast growth factor concentrations in the serum and cerebrospinal fluid of patients with Alzheimer's disease. J. Clin. Neurosci 17, 357–359.

Mason, I.J., 1994. The ins and outs of fibroblast growth factors. Cell 78, 547–552.

Mohan, S.K., Rani, S.G., Yu, C., 2010. The heterohexameric complex structure, a component in the non-classical pathway for fibroblast growth factor 1 (FGF1) secretion. J. Biol. Chem. 285, 15464–15475.

Mohiuddin, L., Femyhough, P., Tomlinson, D.R., 1996. Acidic fibroblast growth factor enhances neurite outgrowth and stimulates expression of GAP-43 and Talpha1 alpha-tubulin in cultured neurons from adult rat dorsal root ganglia. Neurosci. Lett. 215, 111–114.

Mouta, C.C., Landriscina, M., Bellum, S., Prudovsky, I., Maciag, T., 2001. The comparative release of FGF1 by hypoxia and temperature stress. Growth Factors 18, 277–285.

Nagayasu, Y., Ito, J.-i., Nishida, T., Yokoyama, S., 2008. Reactivity of astrocytes to fibroblast growth factor-1 for biogenesis of apolipoprotein E-high density lipoprotein is down-regulated

Please cite this article as: Ito, J., et al., Enhancement of FGF-1 release along with cytosolic proteins from rat astrocytes by hydrogen peroxide, (2013), http://dx.doi.org/10.1016/j.brainres.2013.05.035

by long-time secondary culture. J. Biochem. (Tokyo) 143, 611–616.
Nishida, T., Ito, J.-i., Nagayasu, Y., Yokoyama, S., 2009. FGF-1-induced reactions for biogenesis of apoE-HDL are mediated by Src in rat astrocytes. J. Biochem. 146, 881–886.
Opalenic, S.R., Ding, Q., Mallery, S., Thompson, J.A., 1998. Glutathione depletion associated with the HIV-1 TAT protein mediates the extracellular appearance of acidic fibroblast growth factor. Arch. Biochem. Biophys. 351, 17–26.
Paster, M.D., Garcia-Yebenes, I., RFradejas, N., Perez-Ortiz, J., Mora-Lee, S., Tranque, P., Mro, M.A., Pende, M., Calvo, S., 2009. mTOR/S6 kinase pathway contributes to astrocyte survival during ischemia. J. Biol. Chem. 284, 22067–22078.
Pratico, D., Trojanowski, J., 2000. Inflammatory hypotheses: novel mechanisms of Alzheimer's neurodegeneration and new therapeutic targets. Neurobiol. Aging 21, 441–445.
Pratico, D., Delanty, N., 2000. Oxidative injury in diseases of the central nervous system: focus on Alzheimer's disease. Am. J. Med. 1009, 577–585.
Prudovsky, I., Mandinova, A., Soidi, R., Bagala, C., Graziani, I., Landriscina, M., Tarantini, F., Duarte, M., Bellum, S., Doherty, H., Maciag, T., 2003. The non-classical export routes: FGF1 and IL-1alpha point the way. J. Cell Sci. 116, 4871–4881.
Shin, J.T., Opalenic, S.R., Wehby, J.N., Mahesh, V.K., Jackson, A., Tarantini, F., Maciag, T., Thompson, J.A., 1996. Serum-stavation induces the extracellular appearance of FGF-1. Biochim. Biophys. Acta 1312, 27–38.
Sobue, K., Yamamoto, N., Hodgson, M.E., Yamashiro, K., Tsuruoka, N., Tsuda, T., Katsuya, H., Miura, Y., Asai, K., Kato, T., 1999. Induction of blood–brain barrier properties in immortalized bovine brain endothelial cells by astrocytic factors. Neurosci. Lett. 35, 155–164.
Tada, T., Ito, J.-i., Asai, M., Yokoyama, S., 2004. Fibroblast growth factor 1 is produced prior to apolipoprotein E in the astrocytes after cryo-injury of mouse brain. Neurochem. Int. 45, 23–30.
Tarantini, F., LaVallee, T.M., Jackson, A., Gamble, S., Mouta, C.C., Garfinkel, S., Burgess, B.L., Maciag, T., 1998. The extravesicular domain of synaptotagmin-1 is released with the latent fibroblast growth factor-1 homodimer in response to heat shock. J. Biol. Chem. 1998, 22209–22216.
Thom, D., Powell, A.J., Lloyd, C.W., Rees, D.A., 1977. Rapid isolation of plasma membranes in high yield from cultured fibroblasts. Biochem. J. 168, 187–194.
Tooyama, I., Akiyama, H., McGeer, P.L., Hara, Y., Yasuhara, O., Kimura, H., 1991. Acidic fibroblast growth factor-like immunoreactivity in brain of Alzheimer patients. Neurosci. Lett. 121, 155–158.
Ueno, S., Ito, J.-i., Nagayasu, Y., Furukawa, T., Yokoyama, S., 2002. An acidic fibroblast growth factor-like factor secretedinto the brain cell culture medium upregulates apoE synthesis HDL secretion and cholesterol metabolism in rat astrocytes. Biochim. Biophys. Acta 1589, 261–272.
Wiedlocha, A., Nilsen, T., Wesche, J., Sorensen, V., Malecki, J., Marcinkowska, E., Olsnes, S., 2005. Phosphorylation-regulated nucleocytoplasmic trafficking of internalized fibroblast growth factor-1. Mol. Biol. Cell 16, 794–810.

Please cite this article as: Ito, J., et al., Enhancement of FGF-1 release along with cytosolic proteins from rat astrocytes by hydrogen peroxide, (2013), http://dx.doi.org/10.1016/j.brainres.2013.05.035

Alzheimer's Disease & Parkinsonism

Ito et al., J Alzheimers Dis Parkinsonism 2013, 3:5
http://dx.doi.org/10.4172/2161-0460.1000133

Case Report Open Access

Oxidative Stress and FGF-1 Release from Astrocytes

Jin-ichi Ito*, Jiansheng Gong and Makoto Michikawa

Biochemistry, Graduate School of Medical Sciences, Nagoya City University, Kawasumi 1, Mizuho-cho, Mizuhoku, Nagoya, Japan

Abstract

The brain is an organ to consume highly oxygen and to produce Reactive Oxygen Species (ROS) at high level. ROS facilitate to produce many kinds of peroxide lipids in the lipid-rich brain. Accordingly, it is considered that the brain is an organ to undergo easily oxidative stress. Severe diseases of brain such as Parkinsonism and Alzheimer's disease are seemingly accompanied with oxidative stress. The construction of protection system against oxidative stress is very important to maintain normal neuron function in the brain. We are studying the production and function of Fibroblast Growth Factor 1 (FGF-1) in astrocytes undergoing oxidative stress.

Astrocytes increase FGF-1 release under stressful condition such as oxidative stress and long-term cultured stress. *In vitro* treatment of rat astrocytes with 100 μM Hydrogen Peroxide (H_2O_2) for 10 min enhances the release of FGF-1 along with cytosolic proteins such as HSP90, HSP70, PK-Cδ without inducing apoptosis. The treatment with H_2O_2 enhanced the flow into the cells of exogenous compounds such as trypsin and Rhodamin-phalloidin also, suggesting increase in permeability of plasma membrane in astrocytes treated with H_2O_2. Oxidative stress suppressed transiently cholesterol synthesis and enhanced cholesterol release from the cell surface, resulted in impairment of the cholesterol metabolism. The change of cholesterol metabolism may participate in the increase in membrane permeability in astrocytes undergone oxidative stress. FGF-1 released from rat astrocytes enhances apoE-containing HDL-like lipoproteins (apoE/HDL) generation of astrocytes in the manner of autocrine action. In this review, we describe physiological significance of FGF-1 released from astrocytes stimulated by oxidative stress to relate with generation of apoE/HDL of astrocytes in the brain.

Keywords: Astrocytes; FGF1; ApoE; HDL; Oxidative stress; Cholesterol

Introduction

Glias are known to occupy approximately 10-fold higher population than neurons, and astrocytes are most abundant glial cells in the brain. The population of astrocytes is approximately 1.4-fold as many as that of neurons in the cerebrum. It has been thought that astrocytes function to support structure and distribution of neurons in the brain, regulate molecular transport between the inside and outside of brain through the Blood-Brain Barier (BBB) along with brain capillary endothelial cells, control energy methabolism of neurons, and keep homeostasis of extracellular emvironment of neural cells. Astrocytes has been considered to play subordinate roles from a viewpoint of the brain function to organize neuronal signal networks in the Central Nervous System (CNS). Recentrly, it was found that astrocytes have receptors of various neurotransmitters and release cytokines and transmittors such as glutamate and D-serine as glio-transmitters, sugesting that astrocytes actively function to regulate various information in neuronal signal networks in the CNS [1,2].

There have been increasing reports that astrocytes function to protect the brain against stresses. Oxidative stress reportedly activates calcium/calmodulin-dependent protein kinase II (CaMKII), followed by activation of Apoptosis Signal-regulating Kinase 1 (ASK1) to induce apoptosis in astrocytes [3]. However, it has been found that protein phosphatase 5 (PP5) localizes widely in the brain and inhibits ASK1 activity, resulted in the protection of neurons against oxidative stress [4]. Astrocytes produce and release Glutathione (GSH) and metallothionein to protect neurons against oxidative stress [5-7]. Furthermore, astrocytes secrete ATP and activate a specific ATP receptor, P2Y1, in the autocrine manner, and then enhance the expression and release of Thioredoxin Reductase (TrxR) in/from astrocytes for protection of the brain against oxidative stress [8]. We found recently that astrocytes increase the FGF-1 secretion under oxidative stress which, in turn, stimulated generation of apoE/HDL in an autocrine manner for protection of brain against oxidative stress [9-12]. Thus, astrocytes own many kinds of means for protection of neural cells from oxidative stress.

Production and Release of FGF-1 from Astrocytes Induced by Oxidative Stress

FGF-1 (acidic FGF) is classified into the FGF family and stimulates the proliferation and differentiation of mesodermal and neuroectodermal cells such as fibroblasts and astrocytes, similarly to FGF-2 (basic FGF). FGF-1 was shown to localize in all motor neurons and primary sensory neurons in the mesencephalon and in a small number of glial cells in the white matter [13]. It have been reported that in Alzheimer's disease, some astrocytes prodece FGF-1 in both the gray and white matters [14]. FGF-1 has already been known to contribute to neuron survival, neurite outgrowth, and angiogenesis *in vitro* and *in vivo* [9,15]. Because FGF-1 and FGF-2 have no amino-terminal signal sequence, these factors are considered to be synthesized and to localize in the cytosol and nucleus of FGF-producing cells [16,17]. Accordingly, their release to the extracellular space is unlikely mediated by the classical intracellular transport system through the Endoplasmic Reticulum (ER)/Golgi pathway after their biosynthesis.

The mechanism underlying FGF-1 release is not so much clear at present despite of many previous investigations [18-20]. FGF-1 seems

***Corresponding author:** Jin-ichi Ito, Biochemistry, Graduate School of Medical Sciences, Nagoya City University, Kawasumi 1, Mizuho-cho, Mizuho-ku, Nagoya, Japan, E-mail: jitoh@med.nagoya-cu.ac.jp

Received July 22, 2013; **Accepted** November 15, 2013; **Published** November 22, 2013

Citation: Ito J, Gong J, Michikawa M (2013) Oxidative Stress and FGF-1 Release from Astrocytes. J Alzheimers Dis Parkinsonism 3: 133. doi: 10.4172/2161-0460.1000133

to be released in response to sublethal cell injuries such as oxidative stress, heat shock, hypoxia, and serum starvation [21-24]. Previous reports have shown that FGF-1 is expressed in reactive astrocytes in the brains of patients with Alzheimer's disease, which is known to be associated with chronic inflammation and oxidative stress [25]. We previously observed that the production and release of FGF-1 are enhanced in rat astrocytes under the long-term cultured stress [10]. These lines of evidence suggest that FGF-1 release is enhanced under stressful conditions such as oxidative stress.

We examined *in vitro* whether the release of FGF-1 from the brain-derived astrocytes is actually triggered by oxidative stress [12]. The treatment of rat astrocytes with 100 μM hydrogen peroxide (H_2O_2) for 10 min enhanced FGF-1 release without inducing apoptosis. After the treatment with H_2O_2, the conditioned medium of rat astrocytes cultured in a fresh medium had the FGF-1-like activities, which enhanced cholesterol synthesis, signalings to phosphorylate Akt and ERK, and apoE secretion. The oxidative stress induced by H_2O_2 enhanced the release of cytosolic proteins such as HSP70 and HSP90 in addition to FGF-1, suggesting the release of FGF-1 takes place along with that of cytosolic proteins from astrocytes undergoing oxidative stress (Figure 1). Antioxidants such as ascorbic acid and ebselen suppresses the release of cytosolic proteins induced by H_2O_2 treatment. We examined whether exogeneously added trypsin goes through membrane into cytosol in astrocytes treated with H_2O_2. The treatment with exogenous trypsin decreased the cellular levels of cytosolic proteins such as HSP90, HSP70, PK-Cδ, and Cav-1 1 h or 3 h after the incubation of the cells with H_2O_2, whereas they remained unchanged in the cells without H_2O_2 (Figure 2A). Rhodamin-phalloidin also flowed into the cells 1 h after H_2O_2 treatment and fixation with paraform aldehyde (Figure 2B). These findings suggest that H_2O_2 treatment enhanced permeability of trypsin and Rhodamin-phalloidin, which enhanced proteolysis of cytoplasmic proteins and staining of cellular actin filaments, respectively. These findings suggest that oxidative stress is one of the candidates which triggers FGF-1 release from astrocytes in the brain.

Mechanism Underlying FGF-1 Release from Astrocytes Induced by Oxidative Stress

The addition of lipoproteins such as Low Density Lipoproteins (LDL) canceles H_2O_2-induced release of FGF-1 and cytosolic proteins (Figure 3) [12]. Furthermore, the pretreatment with LDL suppressed exogenous trypsin-induced proteolysis of cytosolic proteins in the H_2O_2-treated rat astrocytes, suggesting that the H_2O_2-induced increase in permeability of exogenous compounds is prevented by the uptake of lipids from exogenous lipoproteins. These findings imply that the increase of membrane permeability induced by H_2O_2 correlates strongly with lipid metabolism.

Interestingly, the treatment with H_2O_2 strongly suppressed apoE secretion from astrocytes, although it did not suppress FGF-1 release, suggesting that oxidative stress may suppress the classical intracellular transport through the ER/Golgi pathway as shown in apoE secretion from astrocytes. This indicates that FGF-1 is released from astrocytes through a process different from the classical secretion pathway. As [^{35}S]-labeled cytosolic proteins of a wide range of molecular weights were released from rat astrocytes treated with 100 μM H_2O_2, it is suggested that the enhancement of FGF-1 release by oxidative stress depends on the mechanism nonspecific to the FGF-1 molecule in astrocytes.

It is interesting also that the release of cytosolic proteins such as HSP90 and HSP70 from astrocytes was enhanced by H_2O_2 at low concentrations, although in other cell types, the release was markedly attenuated in Balb3T3 cells, remained unchanged in bovine endothelium cells, or diminished in HepG2 cells [12]. These findings suggest that astrocytes are more sensitive to H_2O_2 in terms of the release of cytosolic proteins.

The treatment with 100 μM H_2O_2 for 10 min inhibited transiently

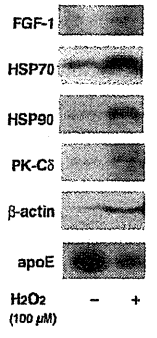

Figure 1: Release of FGF-1 and cytosolic proteins from rat astrocytes treated with hydrogen peroxide without inducing apoptosis. After treatment with 100 μM H_2O_2 for 10 min and incubation in a fresh medium for 16 h, the conditioned medium of rat astrocytes was analyzed by SDS-PAGE and Western blotting for HSP70, HSP90, protein kinase Cδ, β-actin, and apoE. The conditioned medium was incubated with Heparin-Sepharose to concentrate FGF-1 and analyzed for FGF-1 by Western blotting.

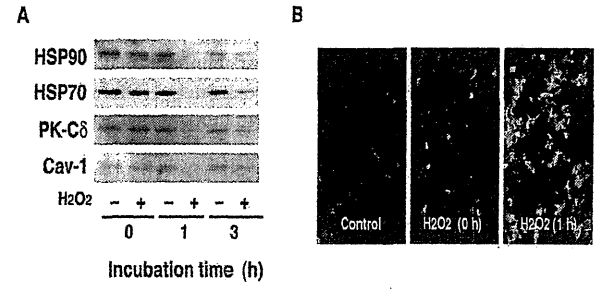

Figure 2: Increase in membrane permeability of rat astrocytes treated with H_2O_2. Change of cytosolic protein level in rat astrocytes was analyzed after the pretreatment with 100 μM H_2O_2 for 10 min and then with exogenous trypsin (A). Inflow of Rhodamin-phalloidin into rat astrocytes was observed 0 or 1 h after the pretreatment with (0 h and 1 h) or without (Control) 100 μM H_2O_2 for 10 min and washing (B).

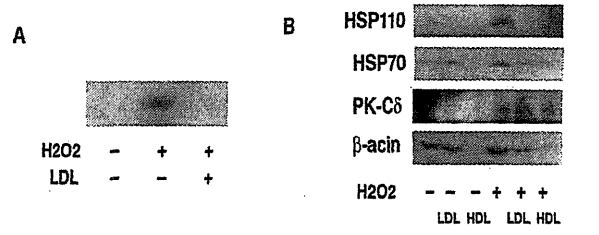

Figure 3: Suppression of H_2O_2-induced release of FGF-1 and cytosolic proteins by exogenous lipoproteins such as LDL and HDL. After the pretreatment with or without LDL or HDL, rat astrocytes were stimulated with or without 100 μM H_2O_2 for 10 min, washed, and incubated in a fresh 0.02% BSA/F-10 medium for the determination of release of FGF-1 (A) or cytosolic proteins (B).

syntheses of cholesterol and sphingomyelin in rat astrocytes and these syntheses were restored approximately 24 h after withdraw of H_2O_2 (Figure 4). The transport and incorporation of metabolically synthesized cholesterol to/in mambrane fraction, especially the membrane lipid rafts, were significantly suppressed by the treatment with H_2O_2 in rat astrocytes. The level of caveolin-1 in membrane lipid rafts was reduced by oxidative stress also. The transport of sphingomyelin to lipid rafts was suppressed as well. These findings suggest that oxidative stress without apoptosis significantly suppresses lipid synthesis and disturbs construction of membrane lipid raft microdomain. Oxidative stress, furthermore, enhances non-specific release of lipids from the cell surface of rat astrocytes (unpublished data), suggesting oxidative stress lowers the lipid level of plasma membrane to make the plasma membrane structure unstable in astrocytes. This may enhance the permeability of cytosolic proteins through the unstable plasma membrane.

Malecki et al. observed that FGF-1 is able to across vesicular membranes from endosomes into the cytosol during G1-phase in the manner dependent on proton pumps [26,27]. FGF-1 appears to be localized in the neural tissue as a high-molecular-weight complex. The complex contains FGF-1 and p40 extravasecular domain of synaptotagmin (Syn)-1, and the brain-derived FGF-1/p40 Syn-1 complex is found to be associated with the calcium-binding protein S100A13 [28,29]. FGF-1 is released as a latent homodimer with the p40 extravasecular domain of Syn-1, as induced by heat-shock stress [30]. These findings indicate that FGF-1 is released as complex forms under stressful conditions. The role of the complex formation of FGF-1 in the release of FGF-1 to extracellular space under stressful condition is as yet unknown [31]. Graziani et al. suggested that the nonclassical pathway of release of FGF-1 and p40 Syn-1 involves the destabilization of the membrane containing acidic phospholipids [32]. We also observed in this study that oxidative stress suppresses syntheses of lipids such as cholesterol and sphingomyelin and incorporation of de novo synthesized lipids to the lipid raft/caveolae domain in the membrane fraction. This may impair the plasma membrane functions and alter lipid raft structure. The sensitive response to oxidative stress to enhance the release of FGF-1 and cytosolic proteins may be a functional feature of astrocytes for protection of the brain from oxidative stress through the released FGF-1.

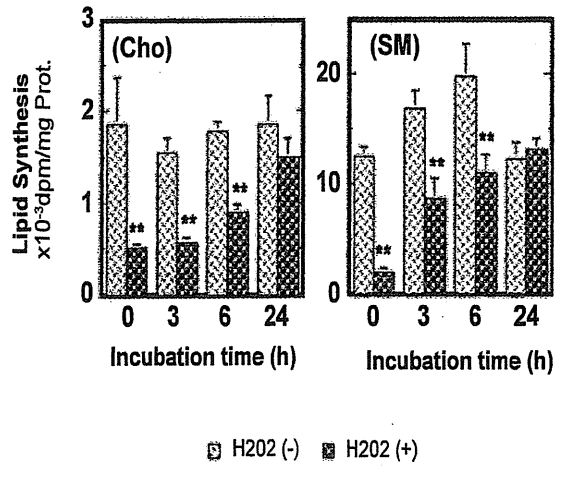

Figure 4: Effect of H_2O_2 on syntheses of lipids such as cholesterol or sphingomyelin in rat astrocytes. After treatment with 100 μM H_2O_2 for 10 min and washing, rat astrocytes were incubated for 0, 3, 6, or 24 h in 0.1% BSA/F-10 medium and then incubated with 14C-acetate in a fresh 0.02% BSA/F-10 for 2 h for lipid synthesis. Lipids were extracted from whole cells and analyzed by thin layer chromatography for cholesterol (Cho) and Sphingo Myelin (SM). The radio activities of cholesterol and sphingomyelin were determined using a liquid scintillation counter. The data points represent the means ± SD, **, $P<0.01$ significantly different from the value of cells treated without H_2O_2.

FGF-1 Enhances apoE/HDL Generation of Astrocytes in a Manner of Autocrine or Paracrine Action

Human apoE is a glycoprotein composed of 299 amino acids with a molecular weight of 34 kDa. ApoE is produced by various types of cells such as macrophages and steroidogenic cells, and the plasma apoE is mainly secreted from the liver. In the brain, the most abundant apolipoprotein is an apoE produced predominantly by astroctes and partly by microglias, and it is secreted for intercellular transport of cholesterol as apoE/HDL with diameters of 10-17 nm in the CNS. As the supply of cholesterol to the CNS is segregated by the BBB from the lipoprotein system in the circulation, apoE/HDL in the brain may be mainly supplied by astrocytes in the brain [33,34].

Endogenous apoE is seemingly transported intracellularly via membrane lipid rafts in astrocytes and generates apoE/HDL through the interaction with ATP-Binding Cassette A1 (ABCA1) [35]. We found that FGF-1 enhances apoE/HDL generation of astrocytes accompanied by the up-regulation of syntheses of apoE and cholesterol, very likely in an autocrine manner [9,10]. It was also observed that the productions of FGF-1 and apoE are increased in the astrocytes around a cryoinjury-induced lesion in the mouse brain [9]. The production of FGF-1 was increased prior to the apoE production in astrocytes after brain injury. Wound healing was substantially delayed in apoE-deficient mice, although the production of FGF-1 was increased in the injured brain also. These findings support the hypothesis that injury and stress induce astrocytes to produce and secrete FGF-1 and up-regulate apoE/HDL generation. It is, thus, possible that astrocytes protect neurons from stress and injury through the FGF-1/apoE/HDL system.

Interestingly, FGF-1 enhances apoE/HDL generation in healthy astrocytes under the stress-less condition but not in unhealthy cells under the stressful condition such as oxidative stress and long-term cultured stress. FGF-1 released from unhealthy astrocytes under some stresses may act on healthy astrocytes to induce apoE/HDL generation through the paracrine action for the protection of neural cells in the brain. In apoE-deficient mouse astrocytes, FGF-1 stimulates cholesterol biosynthesis but not enhancing its release, indicating the cholesterol release is enhanced by FGF-1 dependently on intrtacellular apoE in astrocytes. Suppression of PI3-kinase activity by LY294002 inhibited apoE/HDL secretion and suppression of MAP kinase cascade by U0126, an inhibitor of MEK and ERK, inhibited cholesterol synthesis without suppression of apoE/HDL generation [9]. However, these compounds failed to suppress FGF-1-induced increase of apoE mRNA expression. FGF-1 increases apoE mRNA expression through the increase of mRNA expression of Liver X Receptor α (LXRα) [9]. These findings suggest that FGF-1 upregulates apoE/HDL generation through at least three independent signaling pathways.

Construction of FGF-1/apoE/HDL System of Astrocytes in Alzuheimar's Disease

Tooyama et al. reported that FGF-1 expression increases in the brain of patients with Alzheimer's disease [14]. There, furthermore, is a report that FGF-1 concentration increases in the serum and cerebrospinal fluid of patients with Alzheimer's disease [36]. FGF-1 immunoreactivity shows significantly high level in neurons of Alzheimer's disease brains

except for neurons in entorhinal cortex [37]. These findings suggest the relationship between the progress of Alzheimer's disease and FGF-1 production in the brain. It is very interesting that FGF-1 expression level is increased in reactive astrocytes surrounding senile plaques [38]. These findings indicate that not only neurons but also astrocytes express FGF-1 in the brain. As production of FGF-1 is enhanced in the brain by the injury and oxidative stress, neuroregenerative diseases such as Alzheimer's disease may enhance FGF-1 expression in an affected part of brain. If so, what is a physiological relevance of FGF-1 production in the brain of Alzheimer's disease?

Alzheimer's disease involves chronic inflammatory reactions, oxidative stress, proteasome inhibition, and high cholesterol level in addition to β-amyloid accumulation. Chronic inflammatory reaction is one of important factors to induce Alzheimer's disease to induce neurodegenerative hypothesis of AD inflammatory cytokines such as IFN-γ, TNF-α, and interleukin-1α [39]. These factors may activate and induce reactive astrocytes. Perhaps, FGF-1 production is incresed in the brain during this process as reported by Tooyama et al. [14]. There are many reports regarding the interaction of β-amyloid with apoE but not with FGF-1 [40,41]. We demonstrated that FGF-1 enhances apoE/HDL generation through the increase in production of apoE and cholesterol by three different signal pathways in astrocytes [9]. We, furthermore, reported that the production of FGF-1 is ahead of that of apoE in the mouse brain with cryo-injury. These observations suggest a possibility that FGF-1 enhances apoE/HDL generation in astrocytes in response to increasing production of β-amyloid to protect the brain from the attack of β-amyloid.

ApoE appears to promote the proteolytic degradation of β-amyloid [42]. ApoE is actively able to associate with soluble nonaggregated β-amyloid peptides as scavengers. β-amyloid-associated apoE/HDL binds to apoE receptors and then is internalized in glial and neuronal cells. Internalyzed β-amyloid is degradated via the endosome/lysosomal pathway. Jiang et al. reported that apoE dramatically enhances the endolytic degradation of β-amyloid peptides by neprilysin within microglia [43]. The capacity of apoE to promote β-amyloid degradation is dependent upon the apoE isoform and its lipidation status. ABCA1 is a key protein to influence apoE lipidation [35]. Inactivation of the ABCA1 gene in APP transgenic mice resulted in reduced levels of apoE, so that these mice exhibit a paradoxical elevation of brain β-amyloid peptide levels [44]. FGF-1 enhances not only apoE production but also cholesterol synthesis to upregulate apoE/HDL generation in astrocytes. Accordingly, FGF-1 is considered to have an indirectly important role to enhance clearance of β-amyloid from the brain through enhancing the level of apoE/HDL, which binds β-amyloid peptide. The clinical regulation of FGF-1 expression in the brain, therefore, is expected as a target for β–amyloid therapy.

Conclusion

It was described physiological significance and mechanism of FGF-1 release from astrocytes undergone oxidative stress. The release of cytosolic proteins such as HSP90 and HSP70 along with FGF-1 from astrocytes was greatly induced by the treatment with very low density of H_2O_2 as compared with other cell strains. In this sense, astrocytes have a higher performance of sensor to oxidative stress for cytosolic protein release. The change of cholesterol metabolism induced by oxidative stress contributes to release of cytosolic proteins in astrocytes. The release of cytosolic proteins from astrocytes is accompanied by FGF-1 release and it may be used for protection of neural cells against oxidative stress in the brain. It is possible that the FGF-1 released from stress-loaded astrocytes stimulates healthy astrocytes for the generation of apoE/HDL. The apoE/HDL is thought to function to protect neural cells against oxidative stress and β-amyloid. Thus, astrocytes have roles to remove or reduce β-amyloid peptides through a FGF-1/apoE/HDL system regulated by astrocytes in an autocrine manner.

References

1. Van Horn MR, Sild M, Ruthazer ES (2013) D-serine as a gliotransmitter and its roles in brain development and disease. Front Cell Neurosci 7: 39.
2. Butt AM (2011) ATP: a ubiquitous gliotransmitter integrating neuron-glial networks. Semin Cell Dev Biol 22: 205-213.
3. Liu G, Zhao J, Chang Z, Guo G (2013) CaMKII activates ASK1 to induce apoptosis of spinal astrocytes under oxygen-glucose deprivation. Cell Mol Neurobiol 33: 543-549.
4. Sanchez-Ortiz E, Hahm BK, Armstrong DL, Rossie S (2009) Protein phosphatase 5 protects neurons against amyloid-beta toxicity. J Neurochem 111: 391-402.
5. Wang XF, Cynader MS (2000) Astrocytes provide cysteine to neurons by releasing glutathione. J Neurochem 74: 1434-1442.
6. Dringen R, Pfeiffer B, Hamprecht B (1999) Synthesis of the antioxidant glutathione in neurons: supply by astrocytes of CysGly as precursor for neuronal glutathione. J Neurosci 19: 562-569.
7. Chung RS, Adlard PA, Dittmann J, Vickers JC, Chuah MI, et al. (2004) Neuron-glia communication: metallothionein expression is specifically up-regulated by astrocytes in response to neuronal injury. J Neurochem 88: 454-461.
8. Eftekharpour E, Holmgren A, Juurlink BH (2000) Thioredoxin reductase and glutathione synthesis is upregulated by t-butylhydroquinone in cortical astrocytes but not in cortical neurons. Glia 31: 241-248.
9. Lu R, Ito J, Iwamoto N, Nishimaki-Mogami T, Yokoyama S (2009) FGF-1 induces expression of LXRalpha and production of 25-hydroxycholesterol to upregulate the apoE gene in rat astrocytes. J Lipid Res 50: 1156-1164.
10. Ueno S, Ito J-i, Nagayasu Y, Furukawa T, Yokoyama S (2002) An acidic fibroblast growth factor-like factor secreted into the brain cell culture medium upregulates apoE synthesis, HDL secretion and cholesterol metabolism in rat astrocytes. Biochim Biophys Acta 1589: 261-272.
11. Nagayasu Y, Ito J, Nishida T, Yokoyama S (2008) Reactivity of astrocytes to fibroblast growth factor-1 for biogenesis of apolipoprotein E-high density lipoprotein is down-regulated by long-time secondary culture. J Biochem 143: 611-616.
12. Ito J, Nagayasu Y, Hoshikawa M, Kato KH, Miura Y, et al. (2013) Enhancement of FGF-1 release along with cytosolic proteins from rat astrocytes by hydrogen peroxide. Brain Res 1522: 12-21.
13. Eckenstein FP, Andersson C, Kuzis K, Woodward WR (1994) Distribution of acidic and basic fibroblast growth factors in the mature, injured and developing rat nervous system. Prog Brain Res 103: 55-64.
14. Tooyama I, Akiyama H, McGeer PL, Hara Y, Yasuhara O, et al. (1991) Acidic fibroblast growth factor-like immunoreactivity in brain of Alzheimer patients. Neurosci Lett 121: 155-158.
15. Mohiuddin L, Fernyhough P, Tomlinson DR (1996) Acidic fibroblast growth factor enhances neurite outgrowth and stimulates expression of GAP-43 and T alpha 1 alpha-tubulin in cultured neurones from adult rat dorsal root ganglia. Neurosci Lett 215: 111-114.
16. Mason IJ (1994) The ins and outs of fibroblast growth factors. Cell 78: 547-552.
17. Wiedlocha A, Nilsen T, Wesche J, Sorensen V, Malecki J, et al. (2005) Phosphorylation-regulated nucleocytoplasmic trafficking of internalized fibroblast growth factor-1. Mol Biol Cell 16: 794-810.
18. Carreira CM, LaVallee TM, Tarantini F, Jackson A, Lathrop JT, et al. (1998). S100A13 is involved in the regulation of fibroblast growth factor-1 and P40 synaptotagmin-1 release in vitro. J Biol Chem 273: 22224-22231.
19. Prudovsky I, Mandinova A, Soldi R, Bagala C, Graziani I, et al. (2003) The non-classical export routes: FGF1 and IL-1alpha point the way. J Cell Sci 116: 4871-4881.
20. Mohan SK, Rani SG, Yu C (2010) The heterohexameric complex structure, a component in the non-classical pathway for fibroblast growth factor 1 (FGF1) secretion. J Biol Chem 285: 15464-15475.

21. Jackson A, Friedman S, Zhan X, Engleka KA, Forough R, et al. (1992) Heat shock induces the release of fibroblast growth factor 1 from NIH3T3 cells. Proc Natl Acad Sci U S A 89: 10691-10695.

22. Shin JT, Opalenik SR, Wehby JN, Mahesh VK, Jackson A, et al. (1996) Serum-starvation induces the extracellular appearance of FGF-1. Biochim Biophys Acta 1312: 27-38.

23. Opalenik SR, Ding Q, Mallery SR, Thompson JA (1998) Glutathione depletion associated with the HIV-1 TAT protein mediates the extracellular appearance of acidic fibroblast growth factor. Arch Biochem Biophys 351: 17-26.

24. Mouta Carreira C, Landriscina M, Bellum S, Prudovsky I, Maciag T (2001) The comparative release of FGF1 by hypoxia and temperature stress. Growth Factors 18: 277-285.

25. Takami K, Matsuo A, Terai K, Walker DG, McGeer EG, et al. (1998) Fibroblast growth factor receptor-1 expression in the cortex and hippocampus in Alzheimer's disease. Brain Res 802: 89-97.

26. Malecki J, Wesche J, Skjerpen CS, Wiedlocha A, Olsnes S (2004) Translocation of FGF-1 and FGF-2 across vesicular membranes occurs during G1-phase by a common mechanism. Mol Biol Cell 15: 801-814.

27. Malecki J, Wiedlocha A, Wesche J, Olsnes S (2002) Vesicle transmembrane potential is required for translocation to the cytosol of externally added FGF-1. EMBO J 21: 4480-4490.

28. LaVallee TM, Tarantini F, Gamble S, Carreira CM, Jackson A, et al. (1998) Synaptotagmin-1 is required for fibroblast growth factor-1 release. J Biol Chem 273: 22217-22223.

29. Landriscina M, Bagala C, Mandinova A, Soldi R, Micussi I, et al. (2001) Copper induces the assembly of a multiprotein aggregate implicated in the release of fibroblast growth factor 1 in response to stress. J Biol Chem 276: 25549-25557.

30. Tarantini F, LaVallee T, Jackson A, Gamble S, Mouta Carreira C, et al. (1998) The extravesicular domain of synaptotagmin-1 is released with the latent fibroblast growth factor-1 homodimer in response to heat shock. J Biol Chem 273: 22209-22216.

31. Chapman ER, Davis AF (1998) Direct interaction of a Ca2+-binding loop of synaptotagmin with lipid bilayers. J Biol Chem 273: 13995-14001.

32. Graziani I, Bagalá C, Duarte M, Soldi R, Kolev V, et al. (2006) Release of FGF1 and p40 synaptotagmin 1 correlates with their membrane destabilizing ability. Biochem Biophys Res Commun 349: 192-199.

33. Dietschy JM, Turley SD (2001) Cholesterol metabolism in the brain. Curr Opin Lipidol 12: 105-112.

34. Linton MF, Gish R, Hubl ST, Bütler E, Esquivel C, et al. (1991) Phenotypes of apolipoprotein B and apolipoprotein E after liver transplantation. J Clin Invest 88: 270-281.

35. Wahrle SE, Jiang H, Parsadanian M, Legleiter J, Han X, et al. (2004) ABCA1 is required for normal central nervous system ApoE levels and for lipidation of astrocyte-secreted apoE. J Biol Chem 279: 40987-40993.

36. Mashayekhi F, Hadavi M, Vaziri HR, Naji M (2010) Increased acidic fibroblast growth factor concentrations in the serum and cerebrospinal fluid of patients with Alzheimer's disease. J Clin Neurosci 17: 357-359.

37. Thorns V, Masliah E (1999) Evidence for neuroprotective effects of acidic fibroblast growth factor in Alzheimer disease. J Neuropathol Exp Neurol 58: 296-306.

38. Kimura H, Tooyama I, McGeer PL (1994) Acidic FGF expression in the surroundings of senile plaques. Tohoku J Exp Med 174: 279-293.

39. Niranjan R (2013) Molecular basis of etiological implications in Alzheimer's disease: focus on neuroinflammation. Mol Neurobiol 48: 412-428.

40. Leduc V, Domenger D, De Beaumont L, Lalonde D, Bélanger-Jasmin S, et al. (2011) Function and comorbidities of apolipoprotein e in Alzheimer's disease. Int J Alzheimers Dis 2011: 974361.

41. Fagan AM, Holtzman DM (2000) Astrocyte lipoproteins, effects of apoE on neuronal function, and role of apoE in amyloid-beta deposition in vivo. Microsc Res Tech 50: 297-304.

42. Tokuda T, Matsubara C, Vidal R, Kumar A, Permanne B, et al. (2000) Lipidation of apolipoprotein E influences its isoform-specif interaction with Alzheimer's amyloid beta peptides. Biochem J 348: 359-365.

43. Jiang Q, Lee CY, Mandrekar S, Wilkinson B, Cramer P, et al. (2008) ApoE promotes the proteolytic degradation of Abeta. Neuron 58: 681-693.

44. Hirsch-Reinshagen V, Maia LF, Burgess BL, Blain JF, Naus KE, et al. (2005) The absence of ABCA1 decreases soluble ApoE levels but does not diminish amyloid deposition in two murine models of Alzheimer disease. J Biol Chem 280: 43243-43256.

Citation: Ito J, Gong J, Michikawa M (2013) Oxidative Stress and FGF-1 Release from Astrocytes. J Alzheimers Dis Parkinsonism 3: 133. doi: 10.4172/2161-0460.1000133

Human Molecular Genetics, 2014, Vol. 23, No. 3 **648–656**
doi:10.1093/hmg/ddt451
Advance Access published on September 18, 2013

Altered CpG methylation in sporadic Alzheimer's disease is associated with APP and MAPT dysregulation

Atsushi Iwata[1,2,3,*], Kenichi Nagata[4], Hiroyuki Hatsuta[5], Hiroshi Takuma[6], Miki Bundo[7], Kazuya Iwamoto[3,7], Akira Tamaoka[6], Shigeo Murayama[5], Takaomi Saido[4] and Shoji Tsuji[2]

[1]Department of Molecular Neuroscience on Neurodegeneration, Graduate School of Medicine and [2]Department of Neurology, Graduate School of Medicine, The University of Tokyo, 7-3-1 Hongo Bunkyo-ku, Tokyo 113-8655, Japan [3]Japan Science and Technology Agency, PRESTO, 4-1-8 Honcho Kawaguchi, Saitama 332-0012, Japan [4]Laboratory for Proteolytic Neuroscience, RIKEN BSI, 2-1 Hirosawa, Wako, Saitama 351-0198, Japan [5]Department of Neuropathology, Tokyo Metropolitan Geriatric Hospital, 35-2 Sakaecho, Itabashi, Tokyo 173-0015, Japan [6]Department of Neurology, University of Tsukuba, 1-1-1 Tennodai, Tsukuba, Ibaraki 305-8575, Japan [7]Department of Molecular Psychiatry, Graduate School of Medicine, The University of Tokyo, 7-3-1 Hongo Bunkyo-ku, Tokyo 113-8655, Japan

Received July 25, 2013; Revised September 4, 2013; Accepted September 13, 2013

The hallmark of Alzheimer's disease (AD) pathology is an accumulation of amyloid β (Aβ) and phosphorylated tau, which are encoded by the amyloid precursor protein (APP) and microtubule-associated protein tau (*MAPT*) genes, respectively. Less than 5% of all AD cases are familial in nature, i.e. caused by mutations in *APP*, *PSEN1* or *PSEN2*. Almost all mutations found in them are related to an overproduction of $A\beta_{1-42}$, which is prone to aggregation. While these genes are mutation free, their function, or those of related genes, could be compromised in sporadic AD as well. In this study, pyrosequencing analysis of post-mortem brains revealed aberrant CpG methylation in *APP*, *MAPT* and *GSK3B* genes of the AD brain. These changes were further evaluated by a newly developed *in vitro*-specific DNA methylation system, which in turn highlighted an enhanced expression of *APP* and *MAPT*. Cell nucleus sorting of post-mortem brains revealed that the methylation changes of *APP* and *MAPT* occurred in both neuronal and non-neuronal cells, whereas *GSK3B* was abnormally methylated in non-neuronal cells. Further analysis revealed an association between abnormal *APP* CpG methylation and apolipoprotein E ε4 allele (*APOE* ε4)-negative cases. The presence of a small number of highly methylated neurons among normal neurons contribute to the methylation difference in *APP* and *MAPT* CpGs, thus abnormally methylated cells could compromise the neural circuit and/or serve as 'seed cells' for abnormal protein propagation. Our results provide a link between familial AD genes and sporadic neuropathology, thus emphasizing an epigenetic pathomechanism for sporadic AD.

INTRODUCTION

Alzheimer's disease (AD) is the most prevalent neurodegenerative disease and is pathologically characterized by an accumulation of amyloid β (Aβ) peptide and phosphorylated tau (1). Since the discovery of the gene mutations responsible for familial AD (FAD), namely *PSEN1*, *PSEN2* and *APP*, which encode presenilin 1, 2 and amyloid precursor protein (APP), respectively, huge advances have been made in our understanding of the disease pathomechanism. Pathologically, sporadic AD and FAD are almost identical in terms of abnormal Aβ and phosphorylated tau accumulation, which suggests that the same genes involved in FAD may also play a role in the pathogenesis of sporadic AD; however, no mutations in these genes have been noted in sporadic cases. Indeed, the etiology of sporadic AD, which accounts for >95% of all AD cases, remains largely unknown.

*To whom correspondence should be addressed at: Department of Molecular Neuroscience on Neurodegeneration, Graduate School of Medicine, The University of Tokyo, 7-3-1 Hongo Bunkyo-ku, Tokyo 113-8655, Japan. Tel: 81 358008672; Email: iwata-tky@umin.ac.jp

Recently, it has been shown that an increase in *APP* gene dosage is a rare cause of FAD (2); in these cases, a 1.5-fold increase in the *APP* expression level resulted in early onset AD. In addition, patients with Down syndrome have been known to exhibit AD pathology in their fourth to fifth decades of life; this is noteworthy because those individuals have an extra copy of chromosome 21, where the *APP* gene is located (3). Thus, *APP* expression in Down syndrome patients is also 1.5-fold higher than in normal controls (NCs). These findings provide convincing evidence that AD can be caused by increased *APP* translation due to increased gene dosage; however, whether or not *APP* gene expression is increased in sporadic AD cases remains controversial (4–7). One of the main reasons for this discrepancy may be due to differences in the quality of post-mortem brain samples. For example, RNA can be compromised by a lengthy post-mortem interval and affected by long-term storage conditions. Alternatively, since the brain is a mixture of several different cell types, it may be difficult to extract subtle expression changes that are occurring in only a limited population of certain cells. We previously reported aberrant CpG demethylation associated with alpha-synuclein (*SNCA*) over-expression in the substantia nigra of patients with Parkinson's disease (8). In this study, we also found that the methylation status remained stable for 24 h post-mortem, which provides good rational for studying DNA methylation instead of RNA expression profiles in post-mortem brains.

Herein, we demonstrate that pyrosequencing analysis of post-mortem brains revealed epigenetic changes in *APP*, *MAPT* and *GSK3B* genes in sporadic cases of AD. Additionally, newly developed *in vitro* experiments confirmed the effect of altered methylation on gene expression. Moreover, the increased methylation observed in sporadic AD brains was more prominent in an apolipoprotein ε4 (APOE4)-negative population. Our results shed new light on sporadic AD pathogenesis by revealing a missing link between genes involved in FAD and proteins accumulated in sporadic AD.

RESULTS

We examined age-matched samples from three institutes in Japan (Table 1). The cerebellum, anterior parietal lobe and inferior temporal lobe cortices were analyzed since those areas were available for the majority of cases (Table 2); also, they are important regions for AD neuropathological diagnosis (9,10). We then selected genes of interest related to sporadic AD or FAD (11), including *ACE*, *APOE*, *APP*, *BACE1*, *GSK3B*, *MAPT* and *PSEN1*. CpG islands were located within those genes using a software program (12). Multiple CpGs for each gene were selected, and primer sets were designed for pyrosequencing (Supplementary Material, Table S1). After precise primer calibration (Supplementary Material, Fig. S2) and selection of validated primer sets, small-scale analyses were performed using 15–20 samples from NC and AD temporal lobe samples (Figs 1A–D and 2A–C). Student's *t*-tests revealed several CpGs of interest (Fig. 2D–E), after which we proceeded with a full investigation of those CpGs using all the available samples; this revealed 15 CpGs among 3 different genes that were differentially methylated in AD brains compared with NC brains (Table 3, Fig. 3). Interestingly, statistical significance was mainly observed in temporal lobe samples, while patterns of methylation difference in parietal and cerebellum samples showed at best some resemblance. To test whether these observed differences were specific for AD, we also assessed temporal lobe samples from 50 patients with dementia with Lewy bodies (DLB); this produced similar results to NC, thus confirming that the higher *APP* 60–63 methylation level is an AD-specific phenomenon (Supplementary Material, Fig. S3).

Table 1. Demographics of the postmortem cases analyzed in this study

	NC	AD
Age at death (year old)	76.59 ± 4.506	78.68 ± 7.987
Male%	58	46.5
Brain weight (g)	1262	1185
Post mortem interval (h)	12	14.5
APOE4 (%)	18.84	53.5

AD, Alzheimer's disease; NC, normal control. There were no statistical differences with age at death.

Table 2. Number of samples per regions used in this study

Region	Cerebellum	Parietal	Temporal
NC	71	76	74
AD	45	59	56
Total	126	135	130

Our initial analysis was performed by bulk DNA samples from the cortices, which was comprised of several different cell types, including neuronal, glial and vascular cells. Thus observed finding might be due to alteration of cellular composition, due to selective loss of neurons in the AD brains. To address this, we utilized an established fluorescence-activated cell sorting (FACS) technique (13) in order to enrich neuronal and non-neuronal nucleus separately. Six AD samples and nine NC samples that were representative of high or low methylation status, as determined by previous analyses, were subjected to this procedure. Average NeuN+ events/NeuN- events ratio was 0.593 ± 0.096 in NC and 0.495 ± 0.047 in AD ($P = 0.4493$ by Student's *t*-test). After successful purification of neuronal and non-neuronal nuclei, DNA was extracted. Subsequent pyrosequencing revealed that for *APP* and *MAPT* CpGs, the difference was due to both neurons and non-neuronal cells. Conversely, the difference in *GSK3B* methylation was mainly observed in non-neuronal cells (Fig. 4). These results suggest that aberrant CpG methylation among these genes could play a role in sporadic AD pathology.

Epigenetic alteration without transcriptional change is of little pathomechanistic interest. However, transcriptome analyses using post-mortem brains have inevitable RNA degradation problems that can compromise the result. Thus, we aimed to obtain *in vitro* experimental data that could thoroughly determine the effect of aberrant methylation. In cultured cells, the methylation status of the four regions identified in this study and the expression levels of corresponding genes showed some correlations, but they were not conclusive (Supplementary Material, Fig. S4), possibly because these cell lines are polyploids with huge numbers of chromosomal rearrangements. To overcome this issue, we

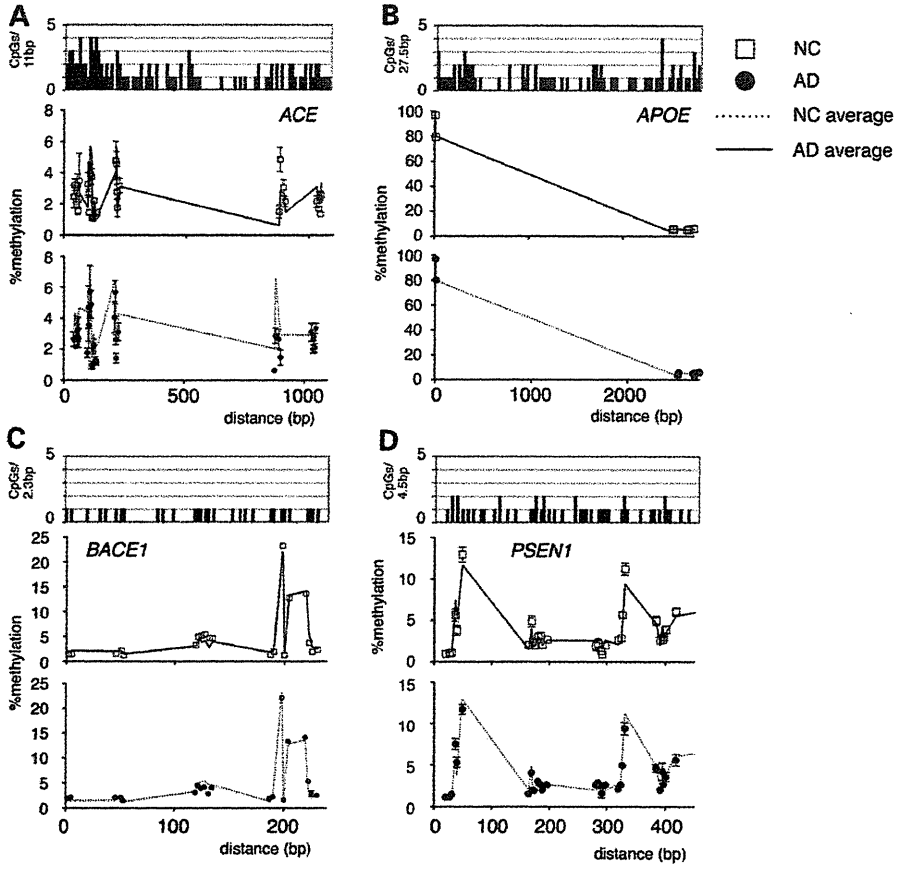

Figure 1. Overview of the methylation status of *ACE*, *APOE*, *BACE1* and *PSEN1* in a small sample group which were obtained before approval of choline esterase inhibitors in Japan. CpG density is shown at the top of the graphs, and the methylation status at the analyzed positions is plotted below. Upper graph panels show normal control (NC) plotted on Alzheimer's disease (AD) average background and the lower panels vice versa. No statistically significant differences were found. (**A**) *ACE*, (**B**) *APOE*, (**C**) *BACE1*, (**D**) *PSEN1*. Open squares: NC with SEM, closed circles: AD with SEM, dotted lines: connecting line of NC average, straight lines: connecting line of AD average. Number of samples used for each groups were 15 in *APP*, *MAPT*, *GSK3B* and 20 in ACE, *APOE*, *BACE1* and *PSEN1*.

established an *in vitro* sequence-specific methylation system using a TAL (transcription activator-like) effector construct fused to the DNA methylase domain of DNMT3a. TALs can be designed to bind specific DNA sequences according to their protein subsequences (14–16). As a control, we generated a methylation-defective DNMT3a mutant V777G construct (17). Among several TAL sequences tested, we found two *APP* CpG 60–63-specific sequences and one *MAPT* 58–62-specific sequence that were effective in altering the methylation level of those two regions. There were no effective TAL sequences for *APP* 88 and *GSKB* 78–82 despite rigorous screening. Although the TAL binding effectiveness was relatively low and the fold methylation change was at most four times compared with the control vector when analyzed by the whole cultured cell population, expression levels of APP and MAPT, as measured by qPCR, were successfully altered along with specific CpG methylation (Fig. 5A–C) and actual methylation level was similar to the values obtained from human samples (Fig. 5D). This result clearly shows that increased *APP* CpG 60–63 methylation was associated with APP expression enhancement, whereas increased *MAPT* 58–62 methylation was associated with MAPT expression suppression, thus leading to the conclusion that epigenetic changes in AD brains, as observed in our study, are associated with an increased expression of both APP and MAPT.

To understand the role of altered methylation in AD pathogenesis, we next tried to correlate other clinical information with CpG methylation. We found that increased methylation of the first half of the *APP* 60–63 CpG region was more prominently observed in *APOE* ε4-negative AD cases (Fig. 6). Moreover, there was some correlation between the methylation status and the *APOE* ε4 gene dosage at *APP* CpGs 60 and 61, although this was not statistically significant due to the small number of *APOE* ε4 homozygotes (Supplementary Material, Fig. S6). Other clinical information such as age at death or sex had no correlation with the methylation level of *APP*, *MAPT* and *GSK3B* (Supplementary Material, Figs S6 and S7).

DISCUSSION

We have previously demonstrated that the methylation level was conserved within 24 h of the post-mortem period (8,18). In

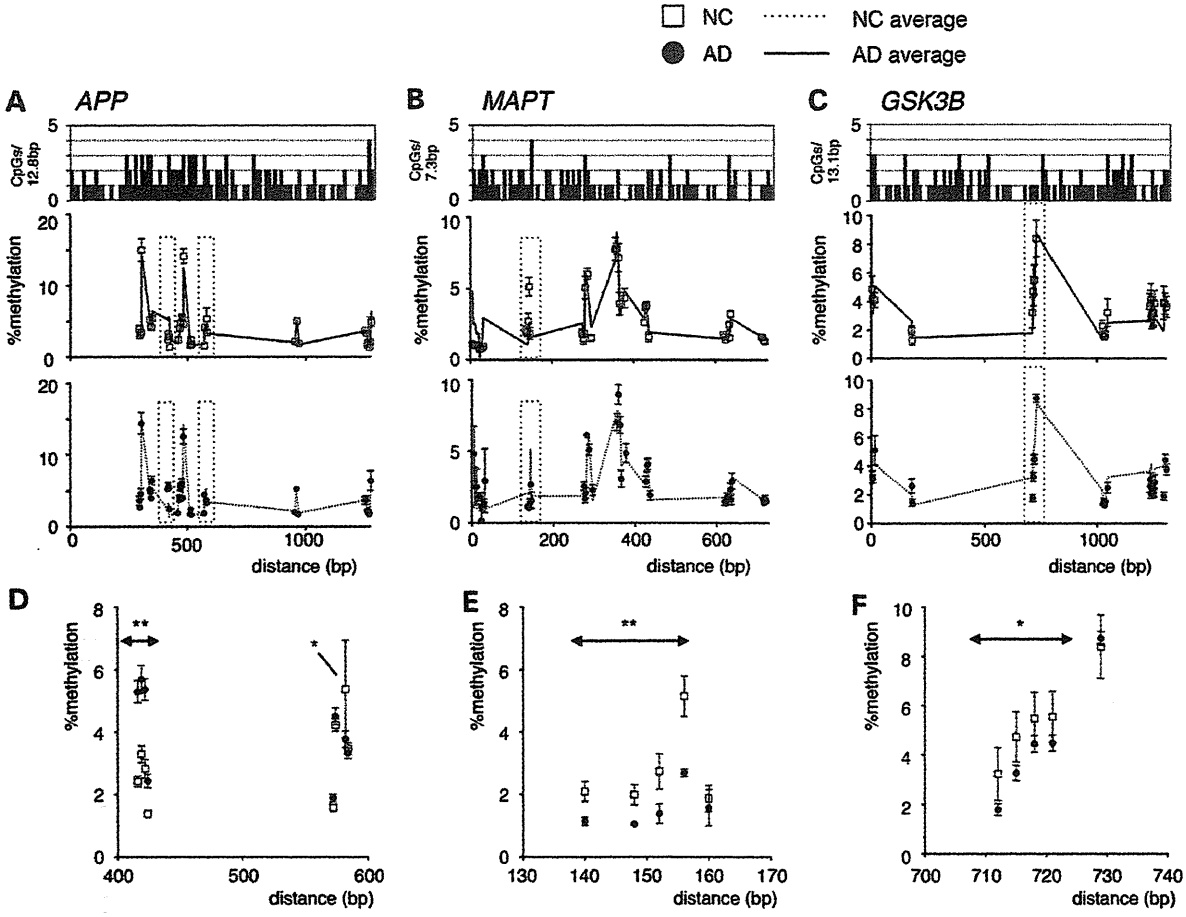

Figure 2. Overview of methylation status of *APP*, *MAPT* and *GSK3B* in a small sample group. (**A**–**C**) CpG density is shown at the top of the graphs, and methylation status at analyzed positions is plotted below. Upper graph panels show NC plotted on AD average background and the lower panels vice versa. Open squares: NC with SEM, closed circles: AD with SEM, dotted lines: connecting line of NC average, straight lines: connecting line of AD average. In each plots, regions of interests that showed statistically significant differences between AD and NC are shown with dotted lines and are magnified in (**D**–**F**). (**A** and **D**) *APP*; (**B** and **E**) *MAPT*; (**C** and **F**) *GSK3B*. $^{*}P < 0.05$, $^{**}P < 0.01$

Table 3. Analyzed genes and the number of CpG sites tested. Statistical analysis revealed five CpG sites in three genes

Gene	Tested CpGs	NC/AD significant CpGs	CpG position
ACE	35	0	
APOE	11	0	
APP	35	5	60–63, 88
BACE1	20	0	
GSK3B	26	5	78–82
MAPT	43	5	58–62
PSEN1	33	0	

addition, since DNA is more stable then RNA, they could reflect the disease process more precisely than transcriptome analysis that can be affected by other factors such as end-stage complications. Thus, our rationale for employing epigenome rather than transcriptome analysis of the post-mortem brain was to avoid the possibility of post-mortem mRNA degradation and transcriptome alterations induced at the agonal stage. Aberrant CpG methylation in AD has been reported; however, there has been no direct link to the pathogenesis of the disease (19). We chose to analyze CpG methylation by pyrosequencing rather than microarray analysis. This is because commercially available microarrays do not cover every single CpG on the genome, and we were concerned with missing CpGs that were of significance. Indeed, past reports on epigenome analysis in either APP CpG island or in AD brains failed to detect significant alteration in AD brains (18,20). In addition, we decided not to employ TA cloning and bisulfite sequencing for large-scale analysis due to its low throughput and cloning bias problems (21,22). However, there were CpGs that could not be assessed in the regions depicted in Figures 1 and 2 due to faulty pyrosequencing primer calibration, there is still a chance that we missed other CpGs of importance.

The analyzed samples were age-matched (Table 1), and the methylation level did not show any correlation with age at death (Supplementary Material, Fig. S7). As usually observed in the AD population, our AD cases were female dominant (Table 1); however, the methylation levels were not affected by sex (Supplementary Material, Fig. S8). Thus, we concluded

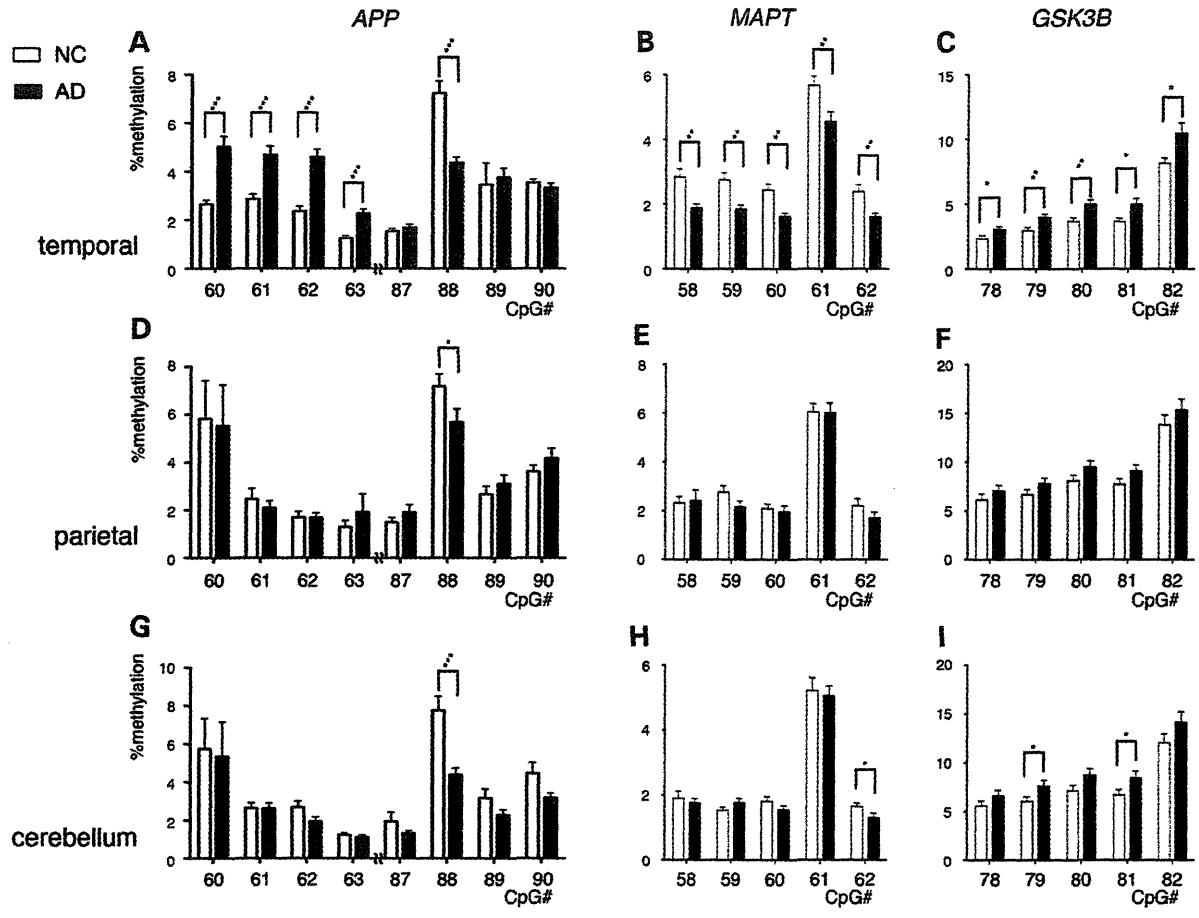

Figure 3. Large-scale analysis of CpG sites of *APP*, *MAPT* and *GSK3B* in three different brain regions. All the samples described in Table 2 was used for analyses. NC, open bars; AD, closed bars. (**A**, **D** and **G**) *APP*; (**B**, **E** and **H**) *MAPT*; (**C**, **F** and **I**) *GSK3B*. (**A**–**C**) Temporal lobe; (**D**–**F**) parietal lobe; (**G**–**I**) cerebellum. Bar = SEM. Two-way ANOVA and Bonferroni's multiple comparison tests revealed statistical significance. $^{*}P < 0.05$, $^{**}P < 0.01$, $^{***}P < 0.001$.

that the results were not biased by age or sex. Direct genome sequencing excluded any single nucleotide polymorphisms in the analyzed regions. Since large numbers of AD patients take choline esterase inhibitors (ChEI), it raises the possibility that such drugs could affect the results. However, our initial screening process (shown in Figs 1 and 2), which was carried out on samples obtained before the approval of donepezil, the first ChEI, in October 1999 in Japan, eliminates this possibility. Thus, we concluded that the CpG alterations observed in AD brains are indeed reflecting the underlying pathological process.

CpGs identified in the analysis were located at different position relative to exons and transcription initiation sites (Fig. 7). CpG methylation at the 5′ promoter region is associated with low transcription factor binding that reduces transcription, whereas CpG methylation in other regions could be associated with enhanced transcriptional activity (23–25). Our *in vitro* experiment data showed higher methylation results had differential effects on gene expression, which is in accordance with these previous findings. Regardless of the CpG methylation alteration, we found all methylation changes in AD brains were associated with an increased expression of *APP* and *MAPT*. Furthermore, our FACS experiment clearly demonstrates that those changes resulted in expression occur in both neuronal and non-neuronal cells. We were initially concerned that significant neuronal loss in AD brains could bias the result. However, comparison of FACS event did not show significant difference in the NeuN+/NeuN− ratio between the NC and AD group, indicating that the neuronal loss did not contribute to epigenetic alteration observed in bulk derived DNA.

Our present finding is of particular interest since increased APP production and MAPT can be directly linked to AD pathogenesis. As for *GSK3B*, we could not determine the effect of hypermethylation in our *in vitro* experiments; however, considering the position of *GSK*3B 78–82 (Fig. 7C), we speculate that hypermethylation may act as a gene expression suppressor. Based on the FACS result, *GSK3B* down-regulation can occur mainly in non-neuronal cells, which in turn might provide some protection against abnormal tau phosphorylation compared with neuronal cells; this is compatible with neuropathological findings that neurofibrillary tangles (NFTs) are seldom found in glial cells of the AD brain while large number of neurons harbors NFTs (26).

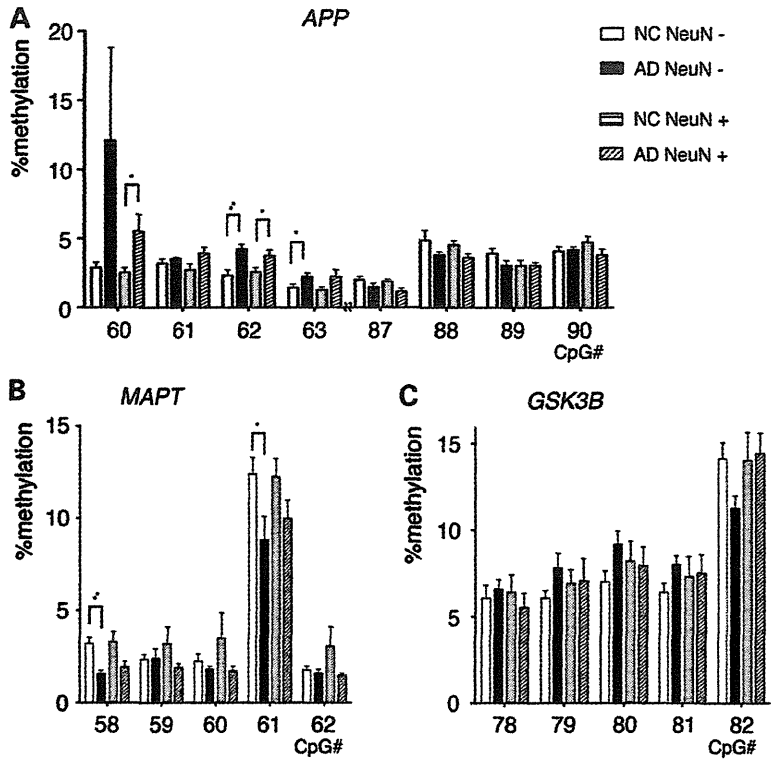

Figure 4. Results of FACS sorting and pyrosequencing analyses. NeuN-positive (+) are neuronal and NeuN-negative (−) are non-neuronal cells. (**A**) *APP*, (**B**) *MAPT*, (**C**) *GSK3B*. Two-way ANOVA and Bonferroni's multiple comparison tests revealed statistical significance. $^{*}P < 0.05$, $^{**}P < 0.01$, $^{***}P < 0.001$.

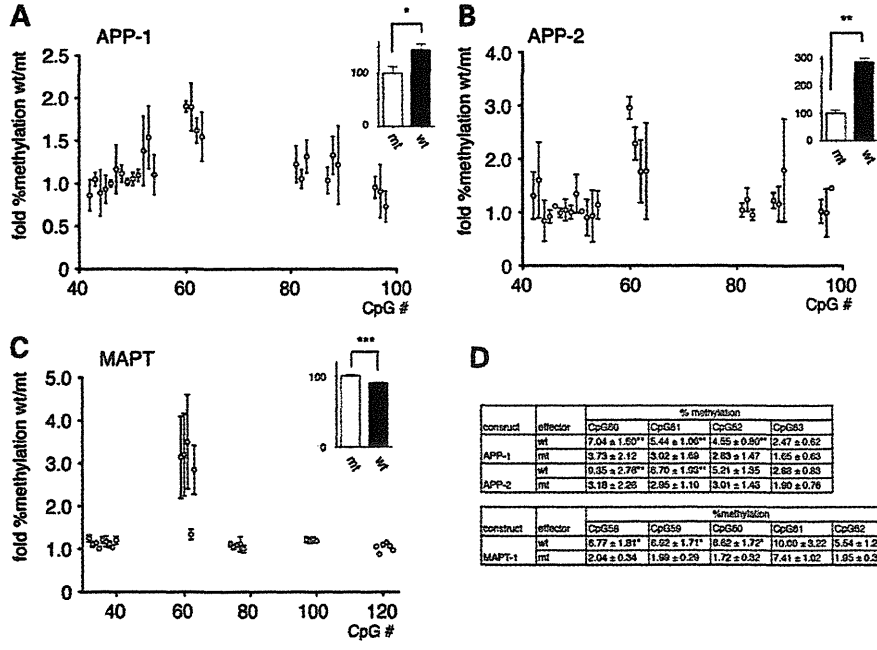

construct	effector	% methylation			
		CpG60	CpG61	CpG62	CpG63
APP-1	wt	7.04 ± 1.60**	5.44 ± 1.06**	4.55 ± 0.80**	2.47 ± 0.62
	mt	3.73 ± 2.12	3.02 ± 1.69	2.83 ± 1.47	1.65 ± 0.63
APP-2	wt	9.35 ± 2.76**	8.70 ± 1.93**	5.21 ± 1.35	2.68 ± 0.83
	mt	3.18 ± 2.26	2.95 ± 1.10	3.01 ± 1.43	1.90 ± 0.76

construct	effector	%methylation				
		CpG58	CpG59	CpG60	CpG61	CpG62
MAPT-1	wt	6.77 ± 1.81*	6.62 ± 1.71*	6.62 ± 1.72*	10.00 ± 3.22	5.54 ± 1.29*
	mt	2.04 ± 0.34	1.99 ± 0.29	1.72 ± 0.32	7.41 ± 1.02	1.95 ± 0.34

Figure 5. Results of TALE-DNMT3a construct transfection. Two different constructs coding *APP* CpGs and one against *MAPT* CpGs were transfected into 293 T cells, which were then incubated for 48 h. RNA and DNA were simultaneously extracted and subjected to qPCR and pyrosequencing. (**A** and **B**) TALE construct against *APP*. (**C**) TALE construct against *MAPT*. Fold % methylation was calculated as the relative value of methylation comparing the wild-type DNMT3a construct against the methylation-defective mutant. Average value from three independent experiments are shown (bar = SEM). Insets are qPCR expression assay results (DNMT V777G mutant = 100). $^{*}P = 0.001$, $^{**}P = 0.0020$, $^{***}P < 0.0001$. (**D**) Actual methylation measurement value (average and SD) of region of interest upon transfection of the constructs are shown. $^{*}P < 0.05$ versus mt, $^{**}P < 0.01$ versus mt.

Since our results are considering relatively low methylation level differences between AD and NC brains, it could raise the concern of pathological significance. For this reason, the results were further analyzed by bisulfite cloning and sequencing of *APP* and *MAPT* in a limited numbers of samples. This revealed some heavily methylated clones among fully unmethylated clones in the AD samples (Supplementary Material, Fig. S8), thus suggesting that a small percentage of abnormally methylated cells are located among normal cells in AD brains. This result supports the aggregation propagation hypothesis that proposes aggregation seed formed somewhere in the brain spreads to other areas (27), that these 'abnormally' methylated cells could serve as seed clones for aggregated protein production. Regional differences observed in this study that most of the methylation differences were observed only in the temporal lobe, where AD pathology usually begins, could also be supportive of the aggregation propagation hypothesis. Our result suggests that there are nearly 2–5% of abnormally methylated cells in the AD temporal cortex. Those cells overproduce APP and MAPT, which could aggregate locally and further spread to adjacent areas of the brain where abnormal seed cells are less abundant. This is further supported by the data shown in Figure 5D that even increase in <10% methylation level can associate with expression alteration, which is due to low transfection and expression efficiency resulting in similar situation observed in the brain that a few abnormally methylated cells are present among normal cells.

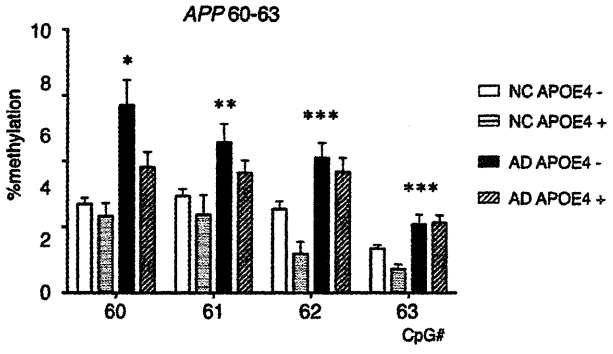

Figure 6. Subgroup analysis of the *APP* methylation status in temporal lobe samples by the presence or absence of APOE ε4 (APOE4). Overall significance was tested by two-way ANOVA and Bonferroni's multiple comparison tests, which revealed a statistically significant positive relationship $^{*}P < 0.0001$ versus NC APOE4−, $P = 0.0333$ versus AD APOE4+, $^{**}P = 0.0015$ versus NC APOE4−, $^{***}P < 0.005$ versus NC APOE4−. We analyzed 64 NC APOE4− 10 NC APOE4+, 27 AD APOE4− and 29 AD APOE4+ cases.

Several genes are considered risk factors for AD; *APOE*, especially the ε4 genotype, confers the strongest risk. This has been shown to affect the disease pathogenesis by impairing Aβ clearance. Approximately 60% of patients with sporadic AD have this allele (28); however, possession of the ε4 allele does not guarantee that an individual will develop AD. Similarly, a significant portion of patients with AD has ε3 alleles, which does not increase the risk of dementia (29). Thus, it is of great interest to identify AD risk factors for the APOE ε4-negative population. Our results suggest a potential role of epigenetic alterations in the disease pathogenesis, especially in the APOE ε4-negative AD population. APOE is a protein related to Aβ clearance, while the E4 protein is reported to be less effective at this task (30); for this reason, it is thought to play a major role in Aβ accumulation in APOE ε4 cases. Thus, in APOE ε4-negative individuals, it may be increased APP production rather than less effective APOE that is related to the disease pathogenesis.

AD is the most prevalent neurodegenerative disease among the elderly and is characterized by the slow progressive decline in memory and executive function, both of which impair the patient's quality of life. As a result of the growing aging population in both developed and developing countries, the number of AD patients will increase dramatically by the year 2050, and the subsequent impact of this on the world economy will be disastrous (31). Existing symptomatic treatments do not change the underlying disease process or halt symptomatic progression (32). Sporadic AD pathogenesis is still unclear, but it is assumed to be somewhat similar to the FAD disease process. Here, we report a novel epigenetic alteration that specifically occurs in sporadic AD patient brains. This result pathomechanistically links FAD and sporadic AD. We hope this finding improves our

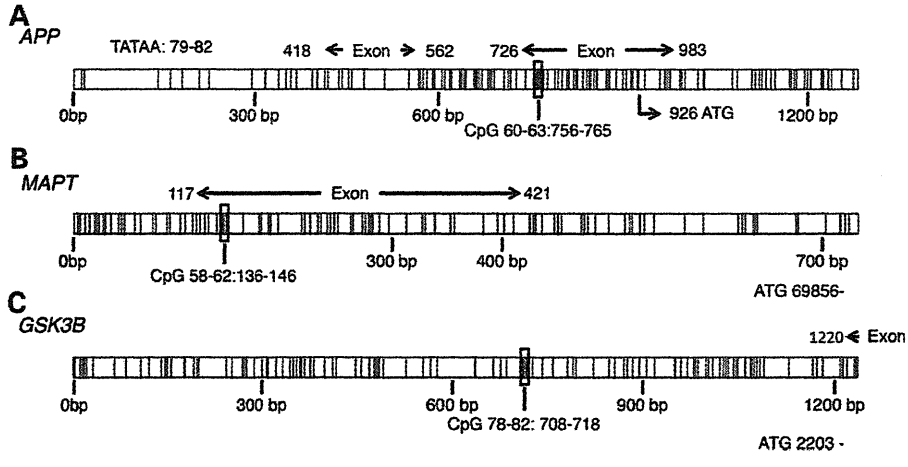

Figure 7. Structures of CpG islands analyzed in this study. Each vertical bar represents a CpG. Regions translated to mRNAs are shown as 'exon', and the first ATG positions are shown. Detected CpG regions are located below the sequences. (**A**) *APP*, (**B**) *MAPT*, (**C**) *GSK*3B.

understanding of AD and can lead to better therapies for this debilitating disease.

MATERIALS AND METHODS

Sample preparation and pyrosequencing

Post-mortem brains were obtained with written consent from patient families, and frozen at −80°C until use. Fifty NC, AD and DLB subjects were obtained from Tokyo Metropolitan Geriatric Hospital brain bank, 16 NC and 10 AD were from University of Tsukuba and 30 NC and 2 AD were from the University of Tokyo. The research was approved by the ethics committee of the University of Tokyo (#2183-6). Unless otherwise noted, gray matter from the inferior temporal lobe, the superior parietal lobe and the cerebellum were excised, and DNA was extracted using the DNeasy Blood and tissue kit (Qiagen, Hilden, Germany), as according to the manufacturer's protocol. After extraction, DNA concentration was measured using a Qubit dsDNA BR assay kit (Invitrogen, Carlsbad, CA, USA). Next, 500 ng genomic DNA was subjected to the Epitect Bisulfite Kit (Qiagen) and eluted with 40 μl buffer. Next, 0.5 μl of the post-bisulfite reaction eluate was amplified via polymerase chain reaction (PCR) with a Pyromark PCR Kit (Qiagen), subjected to pyrosequencing with a Pyromark Q24 analyzer (Qiagen), and the result was analyzed with the Pyromark Q24 software (Qiagen). The list of PCR primers, sequencing primers and analysis settings are shown in Supplementary Material, Table S1. Primer sets for pyrosequencing were designed by the Pyromark Assay Design 2.0 software (Qiagen). EpiTect PCR Control DNA set (Qiagen) was used for primer calibration.

Statistical analyses

Statistical analyses were performed using the Graphpad Prism software (Graphpad Software, La Jolla, CA, USA). Statistical significance was tested by *t*-test and two-way ANOVA with Bonferroni's multiple comparison tests. Correlation analysis was tested by Pearson product-moment correlation coefficient analysis.

Neuropathological diagnosis

According to established criteria by Braak and McKeith (33–35), trained neuropathologists made diagnosis of AD, DLB or NC using hematoxylin–eosin, Nissl and silver staining, as well as immunostainings. Diagnosis of AD was based on Braak stage ≥3 and amyloid stage ≥B. DLB samples were at Lewy body score ≥4, Braak stage ≤3 and amyloid stage ≤B.

CpG island detection

CpG islands were detected using the CpG island searcher software (www.uscnorris.com/cpgislands/) (12).

Quantitative PCR

Cells were cultured under 5% CO_2 and 95% air, and kept at 37°C in ATCC recommended medium conditions. Cultured cells included 293, 293T, BE-(2)-C, H4, HeLa, HeLa-S3, IMR-32, SH-SY5Y and SK-SN which were used in Supplementary Material, Figure S5 experiments. Cells were treated with TRIzol reagent (Invitrogen, Carlsbad, CA, USA) to extract RNA and DNA. A total of 1 μg total RNA per sample was reverse transcribed with Rever-Tra-ACE (Toyobo, Osaka, Japan) and analyzed by a Taqman assay using Hs00902194_m1 (*MAPT*), Hs01552283_m1 (*APP*), Hs01047719_m1 (*GSK*) and Hu GAPDH probe sets (Applied Biosystems, Foster City, CA, USA) in the 7900HT Fast Real-time PCR system (Applied Biosystems). Each individual experiments were assayed in quadruplicate and average values were used for further statistical analysis.

APOE genotyping

APOE genotyping was performed with a Taqman assay using probes C_3084793_20 and C_904973_10 (Applied Biosystems).

FACS nucleus sorting

FACS sorting was performed according to a published protocol (13). One hundred to 200 mg of brain tissue were processed to obtain 100 000–2 000 000 events following NeuN antibody staining.

TALE construct

TALE constructs were made with the TALE toolbox kit (Addgene, Cambridge, MA, USA). The target sequences for *APP* were 5′-TGCCGAGCGGGGTGGGCCGG-3′ and 5′-TGG GCCGGATCAGCTGACTC-3′. The target sequence for *MAPT* was 5′-TTCTCCTCCGGCCACTAGTG-3′. The TALE effector sequence was confirmed by direct sequencing. DNMT3a cDNA (FXC03883) was purchased from Kazusa DNA Research Institute (Kisarazu, Ciba, Japan). The V777G mutation was introduced by PCR. Transfection was performed by Lipofectamine2000 (Lifetechnologies, Carlsbad, CA, USA) following manufacturer's protocol.

SUPPLEMENTARY MATERIAL

Supplementary Material is available at *HMG* online.

ACKNOWLEDGEMENTS

We are grateful for the technical support provided by Yuko Mitani, Yuki Inukai, and Yuko Naramoto. We are grateful to the Support Unit for Bio-Material Analysis, RIKEN BSI Research Resources Center, for the cell sorting.

Conflict of Interest statement. None declared.

FUNDING

This study was supported by JST PRESTO (Kawaguchi, Saitama), the Cell Science Research Foundation (Osaka, Japan), the Ichiro Kanehara Foundation for the Promotion of Medical Sciences and Medical Care (Tokyo, Japan), the

Takeda Science Foundation (Osaka, Japan), Janssen Pharmaceutical K.K. (Tokyo, Japan) and Eisai Co. (Tokyo, Japan).

REFERENCES

1. Karran, E., Mercken, M. and De Strooper, B. (2011) The amyloid cascade hypothesis for Alzheimer's disease: an appraisal for the development of therapeutics. *Nat. Rev. Drug. Discov.*, **10**, 698–712.
2. Rovelet-Lecrux, A., Hannequin, D., Raux, G., Le Meur, N., Laquerriere, A., Vital, A., Dumanchin, C., Feuillette, S., Brice, A., Vercelletto, M. *et al.* (2006) APP Locus duplication causes autosomal dominant early-onset Alzheimer disease with cerebral amyloid angiopathy. *Nat. Genet.*, **38**, 24–26.
3. Wisniewski, K.E., Wisniewski, H.M. and Wen, G.Y. (1985) Occurrence of neuropathological changes and dementia of Alzheimer's disease in Down's syndrome. *Ann. Neurol.*, **17**, 278–282.
4. Golde, T.E., Estus, S., Usiak, M., Younkin, L.H. and Younkin, S.G. (1990) Expression of beta amyloid protein precursor mRNAs: recognition of a novel alternatively spliced form and quantitation in Alzheimer's disease using PCR. *Neuron*, **4**, 253–267.
5. Palmert, M.R., Podlisny, M.B., Golde, T.E., Cohen, M.L., Kovacs, D.M., Tanzi, R.E., Gusella, J.F., Whitehouse, P.J., Witker, D.S., Oltersdorf, T. *et al.* (1990) Analysis of the beta-amyloid protein precursor of Alzheimer's disease: mRNAs and protein products. *Adv. Neurol.*, **51**, 181–184.
6. Koo, E.H., Sisodia, S.S., Cork, L.C., Unterbeck, A., Bayney, R.M. and Price, D.L. (1990) Differential expression of amyloid precursor protein mRNAs in cases of Alzheimer's disease and in aged nonhuman primates. *Neuron*, **4**, 97–104.
7. Harrison, P.J., Wighton-Benn, W.H., Heffernan, J.M., Sanders, M.W. and Pearson, R.C. (1996) Amyloid precursor protein mRNAs in Alzheimer's disease. *Neurodegeneration*, **5**, 409–415.
8. Matsumoto, L., Takuma, H., Tamaoka, A., Kurisaki, H., Date, H., Tsuji, S. and Iwata, A. (2010) Cpg demethylation enhances alpha-synuclein expression and affects the pathogenesis of Parkinson's disease. *PLoS One*, **5**, e15522.
9. Hyman, B.T., Phelps, C.H., Beach, T.G., Bigio, E.H., Cairns, N.J., Carrillo, M.C., Dickson, D.W., Duyckaerts, C., Frosch, M.P., Masliah, E. *et al.* (2012) National Institute on Aging-Alzheimer's Association guidelines for the neuropathologic assessment of Alzheimer's disease. *Alzheimers Dement.*, **8**, 1–13.
10. Montine, T.J., Phelps, C.H., Beach, T.G., Bigio, E.H., Cairns, N.J., Dickson, D.W., Duyckaerts, C., Frosch, M.P., Masliah, E., Mirra, S.S. *et al.* (2012) National Institute on Aging-Alzheimer's Association guidelines for the neuropathologic assessment of Alzheimer's disease: a practical approach. *Acta Neuropathol.*, **123**, 1–11.
11. De Strooper, B., Vassar, R. and Golde, T. (2010) The secretases: enzymes with therapeutic potential in Alzheimer disease. *Nat. Rev. Neurol.*, **6**, 99–107.
12. Takai, D. and Jones, P.A. (2003) The CpG island searcher: a new WWW resource. *In Silico Biol.*, **3**, 235–240.
13. Iwamoto, K., Bundo, M., Ueda, J., Oldham, M.C., Ukai, W., Hashimoto, E., Saito, T., Geschwind, D.H. and Kato, T. (2011) Neurons show distinctive DNA methylation profile and higher interindividual variations compared with non-neurons. *Genome Res.*, **21**, 688–696.
14. Boch, J., Scholze, H., Schornack, S., Landgraf, A., Hahn, S., Kay, S., Lahaye, T., Nickstadt, A. and Bonas, U. (2009) Breaking the code of DNA binding specificity of TAL-type III effectors. *Science*, **326**, 1509–1512.
15. Moscou, M.J. and Bogdanove, A.J. (2009) A simple cipher governs DNA recognition by TAL effectors. *Science*, **326**, 1501.
16. Sanjana, N.E., Cong, L., Zhou, Y., Cunniff, M.M., Feng, G. and Zhang, F. (2012) A transcription activator-like effector toolbox for genome engineering. *Nat. Protoc.*, **7**, 171–192.
17. Gowher, H. and Jeltsch, A. (2002) Molecular enzymology of the catalytic domains of the Dnmt3a and Dnmt3b DNA methyltransferases. *J. Biol. Chem.*, **277**, 20409–20414.
18. Barrachina, M. and Ferrer, I. (2009) DNA Methylation of Alzheimer disease and tauopathy-related genes in postmortem brain. *J. Neuropathol. Exp. Neurol.*, **68**, 880–891.
19. Wang, S.C., Oelze, B. and Schumacher, A. (2008) Age-specific epigenetic drift in late-onset Alzheimer's disease. *PLoS One*, **3**, e2698.
20. Rogaev, E.I., Lukiw, W.J., Lavrushina, O., Rogaeva, E.A. and St George-Hyslop, P.H. (1994) The upstream promoter of the beta-amyloid precursor protein gene (APP) shows differential patterns of methylation in human brain. *Genomics*, **22**, 340–347.
21. Grunau, C., Clark, S.J. and Rosenthal, A. (2001) Bisulfite genomic sequencing: systematic investigation of critical experimental parameters. *Nucleic. Acids. Res.*, **29**, e65.
22. Warnecke, P.M., Stirzaker, C., Song, J., Grunau, C., Melki, J.R. and Clark, S.J. (2002) Identification and resolution of artifacts in bisulfite sequencing. *Methods*, **27**, 101–107.
23. Gius, D., Cui, H., Bradbury, C.M., Cook, J., Smart, D.K., Zhao, S., Young, L., Brandenburg, S.A., Hu, Y., Bisht, K.S. *et al.* (2004) Distinct effects on gene expression of chemical and genetic manipulation of the cancer epigenome revealed by a multimodality approach. *Cancer Cell*, **6**, 361–371.
24. Suzuki, M.M. and Bird, A. (2008) DNA Methylation landscapes: provocative insights from epigenomics. *Nat. Rev. Genet.*, **9**, 465–476.
25. Jones, P.A. (2012) Functions of DNA methylation: islands, start sites, gene bodies and beyond. *Nat. Rev. Genet.*, **13**, 484–492.
26. Lee, V.M. and Trojanowski, J.Q. (1992) The disordered neuronal cytoskeleton in Alzheimer's disease. *Curr. Opin. Neurobiol.*, **2**, 653–656.
27. Frost, B. and Diamond, M.I. (2010) Prion-like mechanisms in neurodegenerative diseases. *Nat. Rev. Neurosci.*, **11**, 155–159.
28. Verghese, P.B., Castellano, J.M. and Holtzman, D.M. (2011) Apolipoprotein E in Alzheimer's disease and other neurological disorders. *Lancet Neurol.*, **10**, 241–252.
29. Liu, C.C., Kanekiyo, T., Xu, H. and Bu, G. (2013) Apolipoprotein E and Alzheimer disease: risk, mechanisms and therapy. *Nat. Rev. Neurol.*, **9**, 106–118.
30. Castellano, J.M., Kim, J., Stewart, F.R., Jiang, H., DeMattos, R.B., Patterson, B.W., Fagan, A.M., Morris, J.C., Mawuenyega, K.G., Cruchaga, C. *et al.* (2011) Human apoE isoforms differentially regulate brain amyloid-beta peptide clearance. *Sci. Transl. Med.*, **3**, 89ra57.
31. Wimo, A. and Price, M. (2010) World Alzheimer Report 2010. *Alzheimer's Disease International*, 1–54.
32. Iwata, A. and Iwatsubo, T. (2013) Disease-modifying therapy for Alzheimer's disease: challenges and hopes. *Neurol. Clin. Neurocience*, **1**, 49–54.
33. Braak, H. and Braak, E. (1991) Demonstration of amyloid deposits and neurofibrillary changes in whole brain sections. *Brain Pathol.*, **1**, 213–216.
34. McKeith, I.G., Galasko, D., Kosaka, K., Perry, E.K., Dickson, D.W., Hansen, L.A., Salmon, D.P., Lowe, J., Mirra, S.S., Byrne, E.J. *et al.* (1996) Consensus guidelines for the clinical and pathologic diagnosis of dementia with Lewy bodies (DLB): report of the consortium on DLB international workshop. *Neurology*, **47**, 1113–1124.
35. Braak, H. and Braak, E. (1991) Neuropathological stageing of Alzheimer-related changes. *Acta Neuropathol.*, **82**, 239–259.